

Response to Reviewer #1

We thank the anonymous reviewer for their helpful comments – we have made several changes to the manuscript in response to their suggestions outlined in red below.

This study describes the characteristics of regional aerosol over the Southeast during the summer of 2013. Through comparisons with the GEOS-Chem model the paper aims to explain the distribution, speciation, and seasonality of PM and AOD in the region. The study provides some new insights into aerosol sources in the region and the August-October transition in concentrations. However, the text over-stretches in some interpretation, and leaves open some key questions. Here are some major issues that the authors should address/correct:

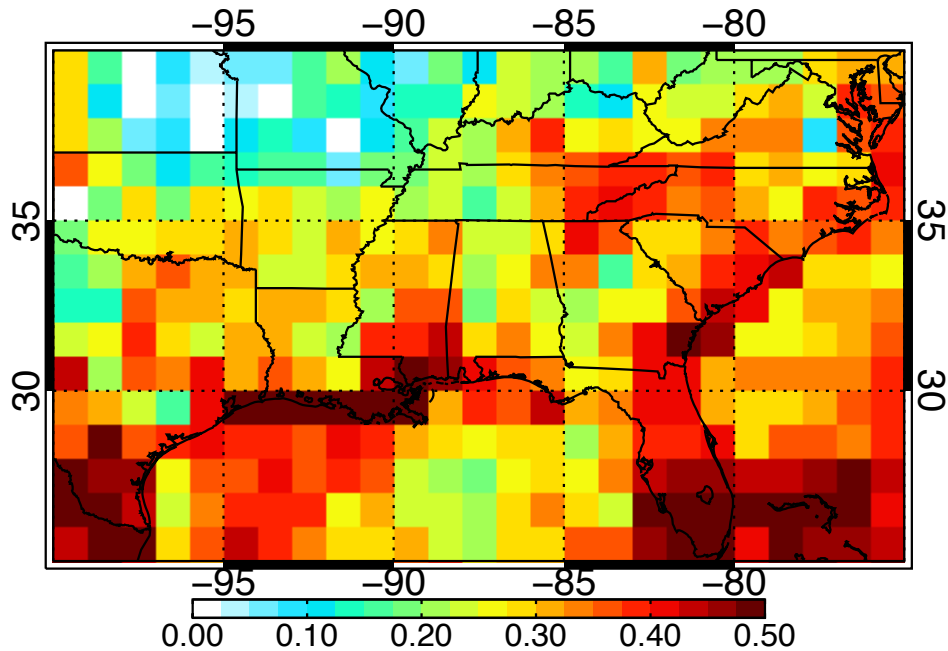
1. The GEOS-Chem model aerosol simulation used in this study is very different from previous published versions (meteorology, ML heights, resolution, emissions, injection heights, chemical mechanism especially with respect to sulfate and OA formation). In order to interpret the results, and particularly comparison with previous GEOS-Chem studies, this study should provide some context for how these changes impact the PM simulation, and where possible (e.g. the impact of changes to sulfate and SOA formation, as well as ML heights) some “before” and “after” comparisons. It’s not clear from the manuscript whether the ability of the model to capture PM concentrations in the Southeast in 2013 is a result of the extensive model modifications and if so, which factor(s) are most important.

We have added quantification of the major changes and their impact on the PM simulation in Section 2.

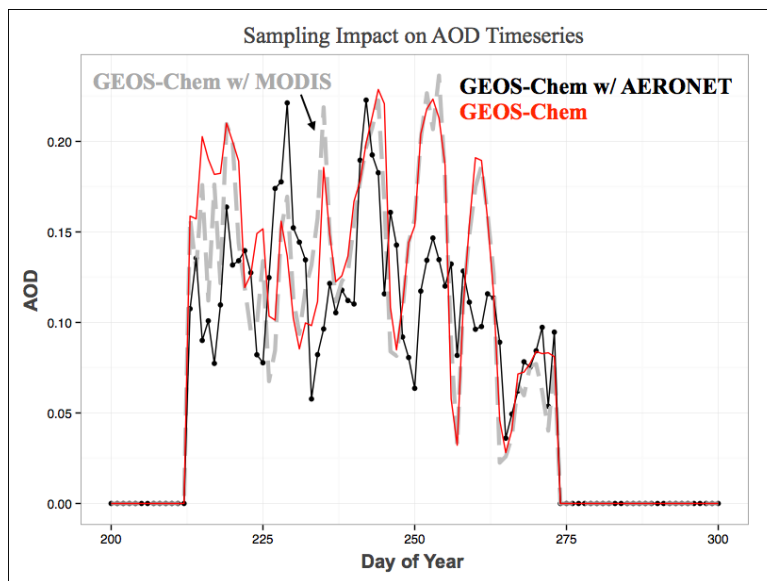
2. Figure 10 and Section 6: The figure shows that the model substantially underestimates MODIS AOD (factor of 2?) in the summer in the SEUS (a seen in Figure 13). This bias should be quantified and discussed in the text, particularly in light of the closer agreement in surface PM and extinction discussed previously (i.e. closure is not achieved, statements on page 17675, line 21-23, page 17676, line 9-10 and all similar statements in the text should be removed). This comparison appears to be in line with the previous results of Goldstein et al., 2009 and Ford and Heald., 2013. The statistics in Figure 10 suggest that both MODIS and GEOS-Chem are both biased low (NMB = -16% vs NMB = -18%) compared to AERONET, whereas the top-left panel of Figure 10 MODIS appears biased high compared to AERONET, not low. This should be resolved. (In addition the sentence on page 17672, line 25-26 is not supported by this analysis).

The model underestimates MODIS AOD by 28% averaged over the Southeast US during August and September 2013 (Figure 10). This is shown below in the difference plot and the information has been added into the text.

GEOS-Chem Percent Low Bias Relative to MODIS AOD August-September 2013



We have moderated our discussion on closure as suggested by the Reviewer. We have added text to explain the apparent discrepancy between the statistics shown inset on Figure 10 and the map. In particular, the statistics compared to AERONET are calculated only when there are collocated and corresponding data for both AERONET and MODIS, whereas the map shows the spatial average for all available data during the mission. This impact of sampling time and location on regional mean AOD is illustrated further in the figure below using GEOS-Chem. The red line shows pure GEOS-Chem output, the black and gray lines when sampling at the available MODIS and AERONET retrievals respectively.



3. The plots and data do not support the conclusion that this model captures the seasonality in AOD in the Southeast. Figure 4 shows ~4-fold increase in observed AOD from winter to summer; whereas the model increase is at most a factor of 2. The text should be extensively revised accordingly, particularly in Section 7 and 8 and the abstract.

We have moderated the text and expanded on the discussion in Section 7 on the underestimate of the seasonal cycle. Our main point however is to focus on using the model to understand how there can be no seasonal cycle in surface PM, but a strong seasonal cycle in AOD.

4. It appears that a highly simplified/tuned non-volatile SOA simulation provides a more reliable simulation of observed OA concentrations and variability than has previously been achieved in field campaign comparisons. What are the implications of this? Does this study suggest that SOA is non-volatile, and models should eliminate the use of partitioning theory and NO_x-dependent yields?

This is an excellent point – we have added commentary to the text as to the implications of the simplified OA parameterization, and added a sentence to the abstract.

Minor Comments

1. Two recent studies (Nguyen et al., ES&T, 2015; Xu et al., PNAS, 2015) have suggested important OA formation mechanisms for the SEUS. How do these relate to the current simulation (are these mechanism included in GEOS-Chem?).

These OA formation mechanisms are not explicitly considered in the GEOS-Chem simulations presented in this study. We now reference Marais et al. (2015) for a more mechanistic GEOS-Chem simulation of OA including consideration of the above references.

2. Page 17656, line 25-26: This sentence should be removed as the manuscript does not support the argument that variation in PBL height is responsible for the seasonality in AOD. (The analysis of Section 7 suggests that the variation in PBL height leads to the simulated seasonality but does not quantify this effect. Furthermore the simulated seasonality underestimates the observed seasonality by a factor of ~2).

Sentence has been removed.

3. Page 17660, lines 27-28: Please clarify - aren't "aqueous aerosols, or cloud processing" included in the sulfate simulation in GEOS-Chem?

We have removed this statement, which was indeed confusing.

4. Page 17661 line 19-page 17662 line 2: This paragraph is confounding. The authors discuss how SOA yields depend on the fate of RO₂, but have assumed that the yield is constant under all conditions, despite their statement that both low-NO_x and high-NO_x

regimes being equally important in this region. This seems like a major limitation of the model simulation, but the implications are not discussed. What conditions do the fixed yields represent and does this represent a lower/upper limit for SOA formation in the region?

This is indeed a limitation of the work and we now refer to Marais et al. (2015) for a more mechanistic GEOS-Chem simulation including different SOA yields in the two regimes.

5. Page 17662, lines 17-18: How does the GEOS-FP meteorology compare with GEOS-5 or MERRA with regards to ML heights? What is the impact of the correction of the ML heights on AOD and PM2.5 simulated in the region?

This information has been added to the text in Section 2.

6. Page 17665, lines 17-19: Is the GEOS-Chem simulation compared to these observations in these studies? If not, please justify this statement.

The comparison numbers of the model to the observations from these studies have been added to the text.

7. Page 17665, lines 27-28: If the trend in OC is driven by a decrease in anthropogenic emissions, why is the downward trend only significant in summer in this analysis?

We don't speculate in the paper on the factors driving the OC trends in summer or winter because we don't feel that our OC simulation is sufficiently mechanistic for this purpose. Again we defer to Marais et al. (2015), which discusses the issue of OC response to long-term trends in SO₂ and NO_x emissions.

8. Page 17667, line 1-2: "these small inconsistent biases may not be significant." – a 20% bias does not seem all that small. Please remove or justify this statement.

Sentence has been removed.

9. Figures 5 and 6 seem inconsistent, particularly with respect to concentrations in the 2-4km altitudes. Figure 6 shows that the median model concentration of sulfate is ~2 times lower than observed aboard the SEAC4RS aircraft, whereas Figure 5 shows much better agreement for mean sulfate. Similarly, median model OA appears lower than observed. The authors should comment on the differences between means and medians and/or choose a consistent approach to their analysis. In light of Figure 6, the statement of page 17668 line 28 seems over-stated.

We thank the reviewer for pointing out the inconsistency for sulfate. Median values are shown in both Figures 5 and 6. However, in Figure 6 the observed vertical profile for sulfate shown is for the SAGA measurement, not the AMS measurement as stated in the text. The figure has been updated accordingly and there are no changes to the conclusions stated in the text (which has also been moderated in tone). The OA values are consistent between Figures 5 and 6.

10. Figure 8: The relationship shown with this cloud of points is not very convincing, and thus this analysis does not seem particularly useful. I recommend removing the figure and shortening the discussion.

The figure has been removed and the text has been revised accordingly – more detailed follow up work on this phenomenon will be explored in Silvern et al. (in prep).

11. Section 6: Why is CALIOP not included in this analysis? It may inform the differences between the CRDS and HSRL, and could provide context for comparing 2013 with previous years. This seems like a major gap in the analysis.

CALIOP data are sparse and interpretation is difficult. We chose not to use them.

12. Page 17673, lines 14-24: Clarify that this mechanism is not included in the current simulation (Figure 12 could be misleading).

Clarification added to the text.

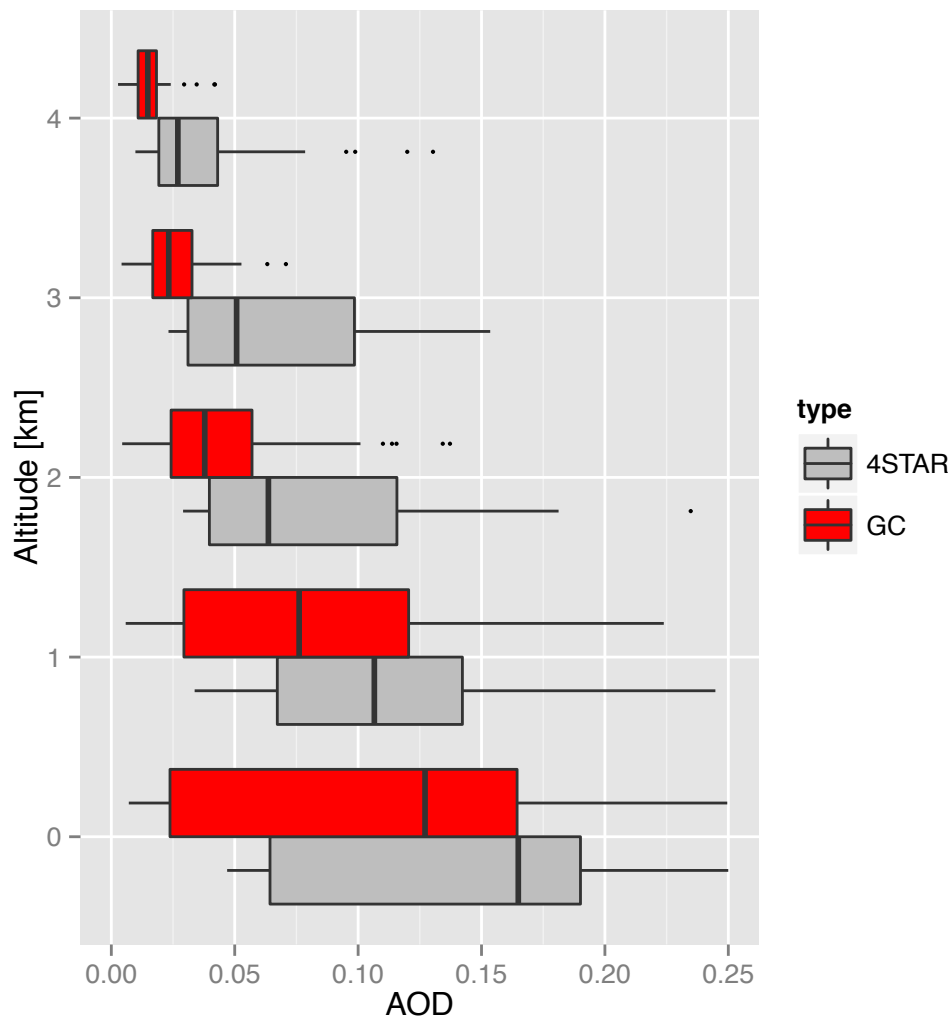
Response to Reviewer #2

We thank the anonymous reviewer for their helpful comments – we have made changes to the manuscript in response to their suggestions outlined in red below.

This paper describes the aerosol characteristics as simulated by the GEOS-Chem model during the NASA SEAC4RS field campaign in 2013. The paper presents comparisons of the aerosol measurements acquired by the NASA DC-8 aircraft and compares the GEOS-Chem simulations with these measurements. Overall the paper provides a very good description of the GEOS-Chem simulations and these comparisons. However, there are a couple of major items the authors need to address before publication. I recommend the authors address these items before publication.

Major 1. The discussion regarding AOD comparisons is confusing. Looking at Figure 10, it looks like the model significantly underestimates AOD relative to MODIS. The MISR comparison looks better but the model still seems to underestimate AOD. The discussion seems to indicate that the GEOS-Chem AOD underestimate is consistent with the aerosol extinction estimate but Figure 9 does not seem to show the same underestimate in aerosol extinction as in AOD. What is the underestimate in extinction relative to both HSRL and the CRDS? Also, why not compare the GEOS-Chem model AOD with the AERONET measurements during the diurnal cycle in at least a few locations? If there is some question as to the ability of the model to represent AOD, it would be good to make some more detailed measurements of AOD with AERONET at various times of the day and a few locations. Also, the DC-8 also deployed the 4STAR instrument, which measured column AOD at many wavelengths; this may help provide additional data for layer AOD comparisons.

Please also see the response to Comment #2 from Reviewer #1. Additional quantification of the model low bias has been added into the text (a low bias of 14.7% relative to CRDS and 16.4% relative to HSRL; 8% low bias relative to MISR; 28% low bias relative to MODIS). Our ability to compare to the AERONET diurnal cycle (i.e. the AOD during the sunlit portion of the day) is limited by the lack of necessary output from the high-resolution simulation results. We will include the 4STAR comparisons, reproduced in the vertical profile shown below at 550 nm (the wavelength of the GEOS-Chem AOD output), in the Supplementary Material. These are the good retrievals (marked with quality flag = 0), which show the above plane AOD. The column low bias (19.1%), taken as the low bias in the lowest 1-km layer, is similar to the low biases discussed previously. The choice of scale truncates some very large observations.



2. There should be more discussion regarding ML heights related to the model. How does the GEOS-Chem derive ML heights? From Richardson number? Aerosol gradients? If the mechanism is different from the lidar measurements, one may expect to see differences depending on location and time of day. Why were the GEOS-Chem heights 30-50% too high before adjustment? What was done to the model to reduce this bias? Does this imply that the model requires external information to constrain the PBL height to satisfactorily estimate PM_{2.5}? How would the GEOS-Chem results been different if these external measurements of PBL height not been available?

Additional discussion of ML heights, how they are defined, and the impact of the ML height adjustment on PM_{2.5} has been added to the text. GEOS-Chem does not directly derive ML height, it is provided from the parent meteorological fields (GEOS-FP) generated by the NASA Global Modeling and Assimilation Office. The ML high bias remains in a more direct comparison when GEOS-FP simulated backscatter profiles are fed into the same processing algorithm for the lidar measurements (Scarino et al., 2014b). The daytime ML height, which is read from the processed GEOS-FP file, was decreased by 40% to correct for this bias. This does imply that a good representation of ML height

is critical for CTM PM_{2.5} applications, but does not necessarily imply that external information is necessary.

Minor

3. Abstract. Why does the model require a missing oxidant?

We elaborate on the need for a missing oxidant for sulfate in Section 2 and deleted that sentence from the abstract (it's not really a take-home message).

4. Abstract. There are statements that say GEOS-chem reproduces observed column aerosol mass with 6%, extinction within 16%, and space-based AOD within 21%. Is GEOS-chem biased higher or lower than these other measurements?

In all cases, the model is biased low – text has been adjusted to make this clearer.

5. Abstract. The abstract needs to mention the performance of GEOS-Chem related to PBL height and this impact on PM_{2.5}.

We prefer not to. The ML bias has to do with the GEOS-FP meteorological fields, not GEOS-Chem proper. This seems like a technical issue to be covered in the text but does not rise to the level of the abstract as a take-home message for the reader.

6. Page 17659, Line 24. Should the Fischer et al., 2014 reference be 2015 instead? I would assume the Fischer reference should use SEAC4RS data.

Fischer et al. (2014) is a general reference about the need to account for fire plume buoyancy in GEOS-Chem.

7. Page 17659, line 29. Note that these are DC-8 flight tracks. It may be appropriate to note that these tracks also extend over other parts of the continental US as well as the Caribbean Sea.

Additional clarification has been added to the text.

8. Page 17662, line 19. The Scarino reference is not listed in the references.

Added to the text.

9. Page 17662, line 22. The Hair et al. reference does not indicate how the HSRL was used to derive ML heights.

See Scarino et al. (2014a), and references therein, which has been added to the reference list.

10. Page 17667, line 29. Since the model requires buoyant injection of forest fire smoke, does this mean the model requires external information to determine the height at which the smoke has been injected?

We now state in the text that we use generic injection heights for extratropical fires based on previous work.

Response to Reviewer #3

We thank the anonymous reviewer for their helpful comments – we have made changes to the manuscript in response to their suggestions outlined in red below.

This paper presents an observation-model integrated analysis of aerosol sources and seasonal variations in Southeast U.S. The high-resolution GEOS-Chem modeling is used as a platform to interpret a variety of aerosol observations from ground, aircraft, and satellite during the SEAC4RS campaign. Short-term trend of aerosol in the last decade is also discussed to some extent. The results from this study are a useful contribution to an improved understanding of aerosol sources and variability/trend in Southeast U.S. The paper is generally well written. I recommend the paper be published after authors adequately address following concerns.

My major concern is about their 40% downward correction of mixing layer (ML) height. First, what is definition of the ML? I thought it is defined as daytime maximum PBL height. However later they try to distinguish ML from PBL (p. 17668, line 26). Or do they define the mixing height just like that based on lidar profiling of aerosol? In any case they need define the ML in the first place and use it consistently throughout the paper.

Additional clarification has been added to the text. GEOS-Chem does not directly derive ML height, it is provided from the parent meteorological fields (GEOS-FP) generated by the NASA Global Modeling and Assimilation Office. The ML height from GEOS-FP is derived from the potential temperature gradient. The ML is not defined as the daytime maximum PBL height – here we define the PBL as the ML + CCL.

Second, it is argued that several studies (Scarino et al., 2015 – which is however not listed in the reference; Millet et al., 2015) have found GEOS-Chem simulated ML is too deep (e.g., 30-50% positive bias) across Southeast U.S. So they reduced the ML height by 40%. However it is not clear to me how they implemented this in the model. Did they adjust some tuning parameters to get the computed ML matching the observation? If they did this way, then they should document those tuning parameters so that other studies may take advantage of the outcome from this study. If not, what did they do exactly? Nevertheless it is important to document how they corrected the ML in the model.

Scarino et al. 2014ab have been added to the reference list. Additional information on how the ML was adjusted has been added to the text (a simple scaling of the variable read in from the offline GEOS-FP meteorological files during daytime hours).

Third, did they compare the GEOS-Chem ML height with some observations? For example, Seidel et al. (JGR, 117, D17106, doi:10.1029/2012JD018143, 2012) derived a climatology of PBL height over U.S. and Europe by using radiosonde observations. Is this PBL climatology useful for their study?

Evaluation of GEOS-FP ML heights against ceilometer measurements during SOAS is presented in Millet et al. (2015). Zhu et al. (in prep.) will present a more thorough comparison to lidar and climatological observations.

Fourth, the 40% downward correction was applied to the GEOS-Chem ML height throughout a year (Figure 13b). Here an inherent assumption is that the modeled ML has a positive bias of ~40% regardless of season. Is this assumption justified? How does this assumption affect their interpretation of the difference in the amplitude of the seasonal cycle between PM_{2.5} and AOD?

This is an excellent question. We make the assumption that the GEOS-FP ML bias applies year round because we lack highly resolved data such as from the lidar during SEAC⁴RS. However, we do not expect this to change the interpretation of the difference in the seasonal cycle amplitude observed between PM_{2.5} and AOD. As an endpoint scenario where there is a 40% reduction in ML height during summer and no reduction in ML height during winter, there is still a 40-50% enhancement (based on Figure 13b) in the ML height during the summer that leads to a difference in magnitude in the seasonal cycles.

Minor changes:

p.17653, 1.10-11: “GEOS-Chem simulation of sulfate requires a missing oxidant, . . .” I don’t quite understand this sentence.

We deleted that sentence from the abstract.

p. 17655, 1.1: Figure 1 shows both summertime and wintertime aerosol trend. But the winter trend is not discussed in main text at all.

We don’t have much to say about the winter trend because it isn’t the focus of our simulation.

p.17657, 1.26: what does “FP” in GEOS-FP stand for?

The FP in GEOS-FP stands for “forward-processing.” Added to the text.

p.17662, 1.1-5: The description of AOD calculation is not right.

We don’t understand the reviewer’s concern. The description is correct. This is how AOD is operationally calculated in GEOS-Chem. Please see: http://www.atmos.colostate.edu/~heald/docs/GEOS_Chem_optics_description.pdf for more details.

p.17671, 1.20: Why use Aqua/MODIS, but not Terra/MODIS?

In our previous work, we found little difference between MODIS AOD on Aqua and Terra and so we chose to focus on the afternoon MODIS data for this analysis.

1 **Manuscript with Tracked Changes**

2

3 **Sources, seasonality, and trends of Southeast US aerosol: an integrated analysis of surface,**
4 **aircraft, and satellite observations with the GEOS-Chem chemical transport model**

5

6 P. S. Kim¹, D. J. Jacob^{1,2}, J. A. Fisher³, K. Travis², K. Yu², L. Zhu², R. M. Yantosca², M. P.
7 Sulprizio², J. L. Jimenez^{4,5}, P. Campuzano-Jost^{4,5}, K. D. Froyd^{4,6}, J. Liao^{4,6}, J. W. Hair⁷, M. A.
8 Fenn⁸, C. F. Butler⁸, N. L. Wagner^{4,6}, T. D. Gordon^{4,6}, A. Welti^{4,6,9}, P. O. Wennberg^{10,11}, J. D.
9 Crouse¹⁰, J. M. St. Clair^{10,*,**}, A. P. Teng¹⁰, D. B. Millet¹², J. P. Schwarz⁶, M. Z. Markovic^{4,6,***},
10 and A. E. Perring^{4,6}

11

12 ¹Department of Earth and Planetary Sciences, Harvard University, Cambridge, MA, USA

13 ²School of Engineering and Applied Sciences, Harvard University, Cambridge, MA, USA

14 ³School of Chemistry, University of Wollongong, Wollongong, New South Wales, Australia

15 ⁴Cooperative Institute for Research in Environmental Sciences, University of Colorado Boulder,
16 Boulder, Colorado, USA

17 ⁵Department of Chemistry and Biochemistry, University of Colorado Boulder, Boulder,
18 Colorado, USA

19 ⁶Chemical Sciences Division, National Oceanic and Atmospheric Administration Earth System
20 Research Laboratory, Boulder, Colorado, USA

21 ⁷NASA Langley Research Center, Hampton, Virginia, USA

22 ⁸Science Systems and Applications, Inc., Hampton, Virginia, USA

23 ⁹Institute for Atmospheric and Climate Science, Swiss Federal Institute of Technology, Zurich,
24 Switzerland

25 ¹⁰Division of Geological and Planetary Sciences, California Institute of Technology, Pasadena,
26 California, USA

27 ¹¹Division of Engineering and Applied Science, California Institute of Technology, Pasadena,
28 California, USA

29 ¹²Department of Soil, Water, and Climate, University of Minnesota, Minneapolis-Saint Paul, MN,
30 USA

31 *now at: Atmospheric Chemistry and Dynamics Laboratory, NASA Goddard Space Flight Center,
32 Greenbelt, MD, USA

33 **now at: Joint Center for Earth Systems Technology, University of Maryland Baltimore County,
34 Baltimore, MD, USA

35 ***now at: Air Quality Research Division, Environment Canada, Toronto, Ontario, Canada

36

37 Correspondence to: P. S. Kim (kim68@fas.harvard.edu)

38

39 **Abstract**

40

41 We use an ensemble of surface (EPA CSN, IMPROVE, SEARCH, AERONET), aircraft
42 (SEAC⁴RS), and satellite (MODIS, MISR) observations over the Southeast US during the
43 summer-fall of 2013 to better understand aerosol sources in the region and the relationship
44 between surface particulate matter (PM) and aerosol optical depth (AOD). The GEOS-Chem
45 global chemical transport model (CTM) with 25 x 25 km² resolution over North America is used
46 as a common platform to interpret measurements of different aerosol variables made at different
47 times and locations. Sulfate and organic aerosol (OA) are the main contributors to surface PM_{2.5}
48 (mass concentration of PM finer than 2.5 μm aerodynamic diameter) and AOD over the Southeast
49 US. OA is simulated successfully with a simple parameterization assuming irreversible uptake of
50 low-volatility products of hydrocarbon oxidation. Biogenic isoprene and monoterpenes account
51 for 60% of OA, anthropogenic sources for 30%, and open fires for 10%. 60% of total aerosol
52 mass is in the mixed layer below 1.5 km, 25% in the cloud convective layer at 1.5-3 km, and 15%
53 in the free troposphere above 3 km. This vertical profile is well captured by GEOS-Chem,
54 arguing against a high-altitude source of OA. The extent of sulfate neutralization ($f =$
55 $[\text{NH}_4^+]/(2[\text{SO}_4^{2-}] + [\text{NO}_3^-])$) is only 0.5-0.7 mol mol⁻¹ in the observations, despite an excess of
56 ammonia present, which could reflect suppression of ammonia uptake by OA. This would explain
57 the long-term decline of ammonium aerosol in the Southeast US, paralleling that of sulfate. The
58 vertical profile of aerosol extinction over the Southeast US follows closely that of aerosol mass.
59 GEOS-Chem reproduces observed total column aerosol mass over the Southeast US within 6%,
60 column aerosol extinction within 16%, and space-based AOD within 8-28% (consistently biased
61 low). The large AOD decline observed from summer to winter is driven by sharp declines in both
62 sulfate and OA from August to October. These declines are due to shutdowns in both biogenic
63 emissions and UV-driven photochemistry. Surface PM_{2.5} shows far less summer-to-winter
64 decrease than AOD due to the offsetting effect of weaker boundary layer ventilation. The
65 SEAC4RS aircraft data demonstrate that AODs measured from space are consistent with surface
66 PM_{2.5}. This implies that satellites can be used reliably to infer surface PM_{2.5} over monthly
67 timescales if a good CTM representation of the aerosol vertical profile is available.
68

Patrick 8/27/2015 11:44 AM

Deleted: GEOS-Chem simulation of sulfate requires a missing oxidant, taken here to be stabilized Criegee intermediates, but which could alternatively reflect an unaccounted for heterogeneous process.

Patrick 8/27/2015 11:44 AM

Deleted: 20

Patrick 8/27/2015 11:44 AM

Deleted: 20

Patrick 8/27/2015 11:44 AM

Deleted: organic aerosol.

Patrick 8/27/2015 11:44 AM

Deleted: 21%.

Patrick 8/27/2015 11:44 AM

Deleted: fundamentally

Patrick 8/27/2015 11:44 AM

Formatted: Font:Bold, No underline, Font color: Custom Color(RGB(26,26,26)), Not Highlight

Patrick 8/27/2015 11:44 AM

Formatted: Indent: First line: 0", Widow/Orphan control, Adjust space between Latin and Asian text, Adjust space between Asian text and numbers

79 **1. Introduction**

80

81 There is considerable interest in using satellite retrievals of aerosol optical depth (AOD)
82 to map particulate matter concentrations (PM) in surface air and their impact on public health (Y.
83 Liu et al., 2004; H. Zhang et al., 2009; van Donkelaar et al., 2010, 2015; X. Hu et al., 2014). The
84 relationship between PM and AOD is a function of the vertical distribution and optical properties
85 of the aerosol. It is generally derived from a global chemical transport model (CTM) simulating
86 the different aerosol components over the depth of the atmospheric column (van Donkelaar et al.,
87 2012, 2013; Boys et al., 2014). Sulfate and organic matter are the dominant submicron aerosol
88 components worldwide (Murphy et al., 2006; Q. Zhang et al., 2007; Jimenez et al., 2009), thus it
89 is important to evaluate the ability of CTMs to simulate their concentrations and vertical
90 distributions. Here we use the GEOS-Chem CTM to interpret a large ensemble of aerosol
91 chemical and optical observations from surface, aircraft, and satellite platforms during the NASA
92 SEAC⁴RS campaign in the Southeast US in August-September 2013. Our objective is to better
93 understand the relationship between PM and AOD, and the ability of CTMs to simulate it, with
94 focus on the factors controlling sulfate and organic aerosol (OA).

95 The Southeast US is a region of particular interest for PM air quality and for aerosol
96 radiative forcing of climate (Goldstein et al., 2009). PM_{2.5} (the mass concentration of particulate
97 matter finer than 2.5 μm aerodynamic diameter, of most concern for public health) is in
98 exceedance of the current US air quality standard, 12 μg m⁻³ on an annual mean basis, in several
99 counties (<http://www.epa.gov/airquality/particlepollution/actions.html>). Concentrations have been
100 decreasing in response to regulation targeted at protecting public health (the Clean Air Act
101 Amendments of 1990). Figure 1 shows the summertime (JJA) and wintertime (DJF) mean
102 concentrations of aerosol components for 2003-2013 from surface monitoring stations in the
103 Southeast US managed by the US Environmental Protection Agency (US EPA, 1999).
104 Summertime sulfate concentrations decreased by 60% over the period while OA concentrations
105 decreased by 40% (Hand et al., 2012b; Blanchard et al., 2013; Hidy et al., 2014). Trends in
106 winter are much weaker. Decreasing aerosol has been linked to rapid warming in the Southeast
107 US over the past two decades (Leibensperger et al., 2012ab).

108 The sulfate decrease is driven by the decline of sulfur dioxide (SO₂) emissions from coal
109 combustion (Hand et al., 2012b), though the mechanisms responsible for oxidation of SO₂ to
110 sulfate are not well quantified. Better understanding of the mechanisms is important because dry
111 deposition competes with oxidation as a sink of SO₂, so that faster oxidation produces more
112 sulfate (Chin and Jacob, 1996). Standard model mechanisms assume that SO₂ is oxidized to

Patrick 8/27/2015 11:44 AM

Deleted: Sulfate

114 sulfate by the hydroxyl radical (OH) in the gas phase and by hydrogen peroxide (H₂O₂) and ozone
115 in clouds (aqueous phase). A model intercomparison by McKeen et al. (2007) for the Northeast
116 US revealed a general failure of models to reproduce observed sulfate concentrations, sometimes
117 by a factor of 2 or more. This could reflect errors in oxidation mechanisms, oxidant
118 concentrations, or frequency of cloud processing. Laboratory data suggest that stabilized Criegee
119 intermediates (SCIs) formed from alkene ozonolysis could be important SO₂ oxidants (Mauldin et
120 al., 2012; Welz et al., 2012), though their ability to produce sulfate may be limited by competing
121 reactions with water vapor (Chao et al., 2015; Millet et al., 2015).

122 The factors controlling OA are highly uncertain. OA originates from anthropogenic,
123 biogenic, and open fire sources (de Gouw and Jimenez, 2009). It is directly emitted as primary
124 OA (POA) and also produced in the atmosphere as secondary OA (SOA) from oxidation of
125 volatile organic compounds (VOCs). Current models cannot reproduce observed OA variability,
126 implying fundamental deficiencies in the model mechanisms (Heald et al., 2011; Spracklen et al.,
127 2011; Tsigaridis et al., 2014). A key uncertainty for air quality policy is the fraction of OA that
128 can be controlled (Carlton et al., 2010), as most of the carbon in SOA is thought to be biogenic in
129 origin. Gas/particle partitioning of organic material depends on the pre-existing aerosol
130 concentration (Pankow et al., 1994; Donahue et al., 2006), so that “biogenic” SOA may be
131 enhanced in the presence of anthropogenic POA and SOA (Weber et al., 2007). The SOA yield
132 from VOC oxidation also depends on the concentration of nitrogen oxide radicals (NO_x = NO +
133 NO₂) (Kroll et al., 2005, 2006; A. Chan et al. 2010; Hoyle et al., 2011; Xu et al., 2014). NO_x in
134 the Southeast US is mostly from fossil fuel combustion and is in decline due to emission controls
135 (Russell et al., 2012), adding another complication in the relationship between OA concentrations
136 and anthropogenic sources. Oxidation of biogenic VOC by the NO₃ radical formed from
137 anthropogenic NO_x is also thought to be an important SOA source in the Southeast US (Pye et al.
138 2010). Reactions of organic molecules with sulfate to form organosulfates may also play a small
139 role (Surratt et al., 2007; Liao et al., 2015).

140 Long-term PM_{2.5} records for the Southeast US are available from the EPA CSN,
141 IMPROVE, and SEARCH networks of surface sites (Malm et al., 1994; Edgerton et al., 2005;
142 Solomon et al., 2014). Satellite measurements of AOD from the MODIS and MISR instruments
143 have been operating continuously since 2000 (Diner et al., 2005; Remer et al., 2005; Levy et al.,
144 2013). Both surface and satellite observations show a strong aerosol seasonal cycle in the
145 Southeast US, with a maximum in summer and minimum in winter (Alston et al., 2012; Hand et
146 al., 2012a; Ford and Heald, 2013). Goldstein et al. (2009) observed that the amplitude of the
147 seasonal cycle of PM_{2.5} measured at surface sites (maximum/minimum ratio of ~1.5; Hand et al.,

148 2012a) is much smaller than the seasonal cycle of AOD measured from space (ratio of ~3-4;
149 Alston et al., 2012). They hypothesized that this could be due to a summertime source of biogenic
150 SOA aloft. Subsequent work by Ford and Heald (2013) supported that hypothesis on the basis of
151 spaceborne CALIOP lidar measurements of elevated light extinction above the planetary
152 boundary layer (PBL). ▾

153 The NASA SEAC⁴RS aircraft campaign in August-September 2013 (Toon et al., 2015)
154 offers a powerful resource for better understanding the factors controlling aerosol concentrations
155 in the Southeast US and the relationship between surface PM and AOD measured from space.
156 The aircraft payload included measurements of aerosol composition, size distribution, and light
157 extinction along with a comprehensive suite of aerosol precursors and related chemical tracers.
158 Flights provided dense coverage of the Southeast US (Figure 2) including extensive PBL
159 mapping and vertical profiling. AERONET sun photometers deployed across the region provided
160 AOD measurements (Holben et al., 1998; http://aeronet.gsfc.nasa.gov/new_web/dragon.html).
161 Additional field campaigns focused on Southeast US air quality during the summer of 2013
162 included SENEX (aircraft) and NOMADSS (aircraft) based in Tennessee (Warneke et al., 2015;
163 http://www.eol.ucar.edu/field_projects/nomadss), DISCOVER-AQ (aircraft) based in Houston
164 (Crawford and Pickering, 2014), SOAS (surface) based in Alabama (<http://soas2013.rutgers.edu>),
165 and SLAQRS (surface) based in Greater St. Louis (Baasandorj et al., 2015). We use the GEOS-
166 Chem CTM with 0.25° x 0.3125° horizontal resolution as a platform to exploit this ensemble of
167 observational constraints by (1) determining the consistency between different measurements, (2)
168 interpreting the measurements in terms of their implications for the sources of sulfate and OA in
169 the Southeast US, (3) explaining the seasonal aerosol cycle in the satellite and surface data, and
170 (4) assessing the ability of CTMs to relate satellite measurements of AOD to surface PM.

171

172 2. The GEOS-Chem CTM

173

174 GEOS-Chem has been used extensively to simulate aerosol concentrations over the US
175 including comparisons to observations (Park et al., 2003, 2004, 2006; Drury et al., 2010; Heald et
176 al., 2011, 2012; Leibensperger et al., 2012a; Walker et al., 2012; L. Zhang et al., 2012; Ford and
177 Heald, 2013). Here we use GEOS-Chem version 9-02 (<http://geos-chem.org>) with detailed
178 oxidant-aerosol chemistry and the updates described below. Our SEAC⁴RS simulation for
179 August-October 2013 is driven by Goddard Earth Observing System – [Forward Processing](#)
180 (GEOS-FP) assimilated meteorological data from the NASA Global Modeling and Assimilation
181 Office (GMAO). The GEOS-FP meteorological data have a native horizontal resolution of 0.25°

Patrick 8/27/2015 11:44 AM

Deleted: As will be shown later, another simple explanation for the difference in seasonal amplitude between satellite AOD and surface PM_{2.5} is the seasonal variation in the PBL height.

186 x 0.3125° (~25 x 25 km²) with 72 vertical pressure levels and 3 h temporal frequency (1 h for
187 surface variables and mixed layer depths). The mixed layer (ML) is defined in GEOS-FP as the
188 unstable surface-based column diagnosed from the potential temperature gradient, with a vertical
189 resolution of ~150 m. It is used in GEOS-Chem for surface-driven vertical mixing following Lin
190 and McElroy (2010). The representation of clouds and their properties, such as liquid water
191 content, are taken from the GEOS-FP assimilated meteorological fields. We use the native
192 resolution in GEOS-Chem over North America and adjacent oceans [130° - 60° W, 9.75° - 60° N]
193 to simulate the August 1 – October 31, 2013 period with a 5-minute transport time step. This is
194 nested within a global simulation at 4° x 5° horizontal resolution to provide dynamic boundary
195 conditions. The global simulation is initialized on June 1, 2012 with climatological model fields
196 and spun up for 14 months, effectively removing the sensitivity to initial conditions.

197 GEOS-Chem simulates the mass concentrations of all major aerosol components
198 including sulfate, nitrate, and ammonium (SNA; Park et al., 2006; L. Zhang et al., 2012), organic
199 carbon (OC; Heald et al., 2006a, 2011; Fu et al., 2009), black carbon (BC; Q. Wang et al., 2014),
200 dust in four size bins (Fairlie et al., 2007), and sea salt in two size bins (Jaegle et al., 2011).
201 Aerosol chemistry is coupled to HO_x-NO_x-VOC-O₃-BrO_x tropospheric chemistry with recent
202 updates to the isoprene oxidation mechanism as described by Mao et al. (2013). Gas/particle
203 partitioning of SNA aerosol is computed with the ISORROPIA II thermodynamic module
204 (Fontoukis and Nenes, 2007), as implemented in GEOS-Chem by Pye et al. (2009). Aerosol wet
205 and dry deposition are described by H. Liu et al. (2001) and L. Zhang et al. (2001) respectively.
206 OC is the carbon component of OA, and we infer simulated OA from OC by assuming OA/OC
207 mass ratios for different OC sources as given by Canagaratna et al. (2015). Model results are
208 presented below either as OC or OA depending on the measurement to which they are compared.
209 Measurements from surface networks are as OC while the aircraft measurements are as OA.

210 Table 1 lists GEOS-Chem emissions in the continental United States (CONUS) for 2013.
211 Values for the Southeast US in August-September are in parentheses. Emissions outside the
212 CONUS are as in Kim et al. (2013) and are used in the global simulation to derive the boundary
213 conditions for the nested grid. US anthropogenic emissions are from the EPA National Emissions
214 Inventory for 2010 (NEI08v2). The NEI emissions are mapped over the 0.25° x 0.3125° GEOS-
215 Chem grid and scaled to the year 2013 by the ratio of national annual totals
216 (<http://www.epa.gov/ttnchie1/trends/>). For BC and SO₂ this implies 3% and 10% decreases from
217 2010 to 2013, but we prescribe instead a 30% decrease for both to better match observed BC
218 concentrations and trends in sulfate wet deposition. Our SO₂ emission adjustment is more
219 consistent with the latest version of the EPA inventory (NEI11v1), which indicates a 34% decline

Patrick 8/27/2015 11:44 AM

Deleted: mixing

Patrick 8/27/2015 11:44 AM

Deleted: In the

Patrick 8/27/2015 11:44 AM

Deleted:), this corresponds to

Patrick 8/27/2015 11:44 AM

Deleted: directly

224 between 2010 and 2013, and with the observed trend in surface concentrations from the SEARCH
225 network, which indicates a ~50% decline in the Southeast US over the same years (Hidy et al.,
226 2014). The NEI08 NH₃ emissions are scaled to 2° x 2.5° gridded monthly totals from the
227 MASAGE inventory, which provides a good simulation of ammonium wet deposition in the US
228 (Paulot et al., 2014).

229 Open fires have a pervasive influence on OA and BC over the US (Park et al., 2007).
230 During SEAC⁴RS, the Southeast US was affected by both long-range transport of smoke from
231 wildfires in the West (Peterson et al., 2014; Saide et al., 2015) and local agricultural fires. We use
232 the Quick Fire Emissions Dataset (QFED2; Darmerov and da Silva, 2013), which provides daily
233 open fire emissions at 0.1° x 0.1° resolution. Diurnal scale factors, which vary by an order of
234 magnitude between midday and evening and peak at 10-19 local time, are applied to the QFED2
235 daily emissions following recommendations from the Western Regional Air Partnership (WRAP,
236 2005) as in Saide et al. (2015). Following previous results from Turquetty et al. (2007) and
237 Fischer et al. (2014) for extratropical fires, we inject 35% of fire emissions above the boundary
238 layer between 680 and 450 hPa to account for plume buoyancy.

239 Biogenic VOC emissions are from the MEGAN2.1 inventory of Guenther et al. (2012)
240 implemented in GEOS-Chem as described by Hu et al. (2015). Isoprene emissions are decreased
241 by 15% to better match SEAC⁴RS observations of isoprene and formaldehyde concentrations and
242 surface fluxes (Travis et al., 2015; Wolfe et al., 2015; Zhu et al., 2015). Figure 2 shows the
243 SEAC⁴RS DC-8 flight tracks superimposed on the distribution of isoprene emissions. Total
244 emissions over the Southeast US (domain outlined in Figure 2) during the 2-month SEAC⁴RS
245 period were 2.2 Tg C for isoprene and 0.5 Tg C for monoterpenes. Monoterpene emissions did
246 not exceed isoprene emission anywhere.

247 Sulfate was too low in our initial simulations of the SEAC⁴RS observations. We
248 addressed this problem by including SCIs as additional SO₂ oxidants in the model as previously
249 implemented in GEOS-Chem by Pierce et al. (2013). This increased mean sulfate over the
250 Southeast US by 50% and improved simulation of the SO₂/sulfate ratio (Section 4). Oxidation of
251 isoprene and monoterpenes provides a large source of SCIs in the Southeast US in summer. Sipila
252 et al. (2014) estimated SCI molar yields from ozonolysis of 0.58 ± 0.26 from isoprene, 0.15 ±
253 0.07 from α-pinene, and 0.27 ± 0.12 from limonene. Sarwar et al. (2014) previously found that
254 simulation of sulfate with the CMAQ CTM compared better with summertime surface
255 observations in the Southeast US when SCI + SO₂ reactions were included in the chemical
256 mechanism. However, production of sulfate from SCI chemistry may be severely limited by
257 competition for SCIs between SO₂ and water vapor and depends on the respective reaction rate

Patrick 8/27/2015 11:44 AM

Deleted: We

Patrick 8/27/2015 11:44 AM

Deleted: (Turquetty et al., 2007; Fischer et al., 2014).

Patrick 8/27/2015 11:44 AM

Deleted: significantly reduced the simulated

Patrick 8/27/2015 11:44 AM

Deleted: bias

Patrick 8/27/2015 11:44 AM

Deleted: moderately

Patrick 8/27/2015 11:44 AM

Deleted: the correlation with observed sulfate in addition to providing a better representation

266 constants (Welz et al., 2012; J. Li et al., 2013; Newland et al., 2014; Sipila et al., 2014; Stone et
267 al., 2014). Here we use SCI chemistry from the Master Chemical Mechanism (MCMv3.2; Jenkins
268 et al., 1997; Saunders et al., 2003) with the SCI + SO₂ and SCI + H₂O rate constants from Stone
269 et al. (2014), using CH₂OO as a proxy for all SCIs, such that the SCI + SO₂ pathway dominates.
270 This would not be the case using the standard SCI + H₂O and significantly slower (~1000x) SCI
271 + SO₂ rate constants in MCM (Millet et al., 2015) or if reaction with the water vapor dimer is
272 important (Chao et al., 2015). Given these crude approximations coupled with the uncertain SCI
273 kinetics, the simulated SCI contribution to SO₂ oxidation can be viewed as a proxy for missing
274 oxidant or insufficient cloud processing in GEOS-Chem.

275 A number of mechanisms of varying complexity have been proposed to model OA
276 chemistry (Donahue et al., 2006; Henze et al., 2006; Ervens et al., 2011; Spracklen et al., 2011;
277 Murphy et al., 2012; Barsanti et al., 2013; Hermansson et al., 2014). These mechanisms tend to
278 be computationally expensive and have little success in reproducing the observed variability of
279 OA concentrations (Tsigaridis et al., 2014). The standard semi-volatile partitioning treatment of
280 OA in GEOS-Chem v9.02 (Pye et al., 2010) underestimates SEAC⁴RS observations several-fold.

281 Here we use a simple linear approach to simulate five components of OA – anthropogenic POA
282 and SOA, open fire POA and SOA, and biogenic SOA. Anthropogenic and open fire POA
283 emissions are from the NEI08 and QFED2 inventories described above. For anthropogenic and
284 open fire SOA, we adopt the Hodzic and Jimenez (2011) empirical parameterization that assumes
285 irreversible condensation of the oxidation products of VOC precursor gases (AVOC and BBVOC
286 respectively). AVOCs and BBVOCs are emitted in proportion to CO, with an emission ratio of
287 0.069 g AVOC (g CO)⁻¹ (Hayes et al., 2014) and 0.013 g BBVOC (g CO)⁻¹ (Cubison et al., 2011).
288 They are both oxidized by OH in the model with a rate constant of 1.25 x 10⁻¹¹ cm³ molecule⁻¹ s⁻¹
289 to generate SOA. This approach produces amounts of SOA and timescales of formation
290 consistent with field measurements at many locations (de Gouw and Jimenez, 2009; Hodzic and
291 Jimenez, 2010; Cubison et al., 2011; Jolleys et al., 2012; Hayes et al., 2014).

292 We assume biogenic SOA to be produced with a yield of 3% from isoprene and 5% from
293 monoterpenes, formed at the point of emission. Laboratory studies have shown that different
294 biogenic SOA formation mechanisms operate depending on the NO concentration, which
295 determines the fate of the organic peroxy radicals (RO₂) produced from VOC oxidation (Kroll et
296 al., 2005, 2006; A. Chan et al., 2010; Xu et al., 2014). In the high-NO pathway the RO₂ radicals
297 react with NO, while in the low-NO pathway they react with HO₂, other RO₂ radicals, or
298 isomerize. During SEAC⁴RS the two pathways were of comparable importance (Travis et al.,
299 2015). We use four separate tracers in the model to track SOA formed from isoprene and

Patrick 8/27/2015 11:44 AM

Deleted: an

Patrick 8/27/2015 11:44 AM

Deleted: that is missing in our current chemical mechanism and that could come from SCIs, aqueous aerosols,

Patrick 8/27/2015 11:44 AM

Deleted: appear to

Patrick 8/27/2015 11:44 AM

Deleted: only limited

Patrick 8/27/2015 11:44 AM

Deleted: regime

Patrick 8/27/2015 11:44 AM

Deleted: regime

Patrick 8/27/2015 11:44 AM

Deleted: regimes

309 monoterpenes via the high- and low-NO pathways. This tracer separation is purely diagnostic as
310 the SOA yields are assumed [here](#) to be the same in both pathways. The SOA is apportioned to the
311 high- or low-NO tracer by the fraction of RO₂ reacting with NO at the point and time of emission.
312 [A more mechanistic GEOS-Chem simulation of SOA in SEAC⁴RS including NO_x-dependent](#)
313 [yields and comparison to semi-volatile partitioning theory is reported by Marais et al. \(2015\).](#)

314 GEOS-Chem computes the AOD for each aerosol component i by summing the optical
315 depths over all vertical model layers $L = [1, \dots, n]$:

316

$$317 \quad \text{AOD} = \sum_i \sum_{L=1}^n \alpha_i(L) M_i(L) \quad [1]$$

318

319 where $\alpha_i(L)$ and $M_i(L)$ are respectively the component mass extinction efficiency ($\text{m}^2 \text{g}^{-1}$) and
320 partial column mass (g m^{-2}) for level L . The α_i values are pre-calculated for selected wavelengths
321 using a standard Mie scattering algorithm. The algorithm assumes specified aerosol dry size
322 distributions and optical properties from the Global Aerosol Data Set (GADS; Koepke et al.,
323 1997), with updates by Drury et al. (2010) on the basis of summer observations from the ICARTT
324 aircraft campaign over the eastern US. The mass extinction efficiencies are then adjusted for
325 hygroscopic growth as a function of the local relative humidity (RH), following R. Martin et al.
326 (2003). The total AOD is reported here at 550 nm and is the sum of the contributions from all
327 aerosol components. Comparison of dry aerosol size distribution and hygroscopic growth show
328 good general agreement with observations similar to Drury et al. (2010) (Supplementary
329 Material).

330 Comparison of GEOS-FP ML heights with lidar and ceilometer data from SEAC⁴RS,
331 SOAS, and DISCOVER-AQ indicates a 30-50% positive bias across the Southeast US in daytime
332 (Scarino et al., [2014b](#); Millet et al., 2015). We decrease the daytime GEOS-FP ML heights by
333 40% in our simulation to correct for this bias. [This increases simulated surface PM_{2.5} by 15-25%.](#)
334 During SEAC⁴RS, ML heights were measured by the NASA-Langley High Spectral Resolution
335 Lidar (HSRL; Hair et al., [2008](#), [Scarino et al., 2014a](#)) on the basis of aerosol gradients under
336 [clear-sky conditions](#). After correction, the modeled ML height is typically within 10% of the
337 HSRL data along the SEAC⁴RS flight tracks, with a mean daytime value (± 1 standard deviation)
338 of 1690 ± 440 m in the HSRL data and 1530 ± 330 m in the model (Zhu et al., 2015). The
339 daytime ML was typically capped by a shallow cloud convective layer (CCL) extending up to
340 about 3 km, capped in turn by a subsidence inversion and the free troposphere above. When
341 giving column statistics we will refer to the ML as below 1.5 km and the CCL as between 1.5 and
342 3 km.

Patrick 8/27/2015 11:44 AM

Deleted: 2015

Patrick 8/27/2015 11:44 AM

Deleted: 2008).

345 Several companion papers apply the same GEOS-Chem model configuration as described
346 here to other analyses of the SEAC⁴RS data focused on gas-phase chemistry. These include
347 investigation of the factors controlling ozone in the Southeast US (Travis et al., 2015), isoprene
348 chemistry and the formation of organic nitrates (Fisher et al., 2015), validation of satellite HCHO
349 data as constraints on isoprene emissions (Zhu et al., 2015), and sensitivity ~~of~~ model
350 concentrations and processes to grid resolution (K. Yu et al., 2015). These studies include
351 extensive comparisons to the gas-phase observations in SEAC⁴RS. Our focus here will be on the
352 aerosol observations.

353

354 3. Surface Aerosol Concentrations

355

356 We begin by evaluating the simulation of PM_{2.5} and its components against ground
357 observations. Total PM_{2.5} is measured gravimetrically at 35% RH at a large number of EPA
358 monitoring sites (Figure 3). Filter-based measurements of PM_{2.5} composition are taken every
359 three days at surface networks including the EPA CSN (25 sites in the study domain marked in
360 Figure 2, mostly in urban areas), IMPROVE (15 sites, mostly in rural areas), and SEARCH (5
361 sites, urban and suburban/rural). These three networks all provide 24-h average concentrations of
362 the major ions (SNA), carbon species (BC and OC), and dust, though there are differences in
363 protocols (Edgerton et al., 2005; Hidy et al., 2014; Solomon et al., 2014), in particular with
364 respect to OC artifact correction. The IMPROVE and SEARCH OC are both blank-corrected but
365 in different ways (Dillner et al., 2009; Chow et al., 2010), while CSN OC is uncorrected. We
366 apply a constant 0.3 μg m⁻³ background correction to the CSN OC data as in Hand et al. (2012a).
367 The resulting CSN OC measurements are within 1% of SEARCH and 44% higher than
368 IMPROVE when averaged across the Southeast US. When necessary, OA is inferred from the OC
369 filter samples using an OA/OC mass ratio of 2.24 as measured in the boundary layer during
370 SEAC⁴RS by an aerosol mass spectrometer (AMS) onboard the DC-8 aircraft (Section 4). We do
371 not discuss sea-salt concentrations as they make a negligible contribution to PM_{2.5} inland (< 0.1
372 μg m⁻³ averaged across the EPA networks).

373 Figure 3 shows mean August-September 2013 PM_{2.5} at the EPA sites and compares to
374 GEOS-Chem values. Concentrations peak over Arkansas, Louisiana, and Mississippi,
375 corresponding to the region of maximum isoprene emission in Figure 2. The spatial distribution
376 and composition of PM_{2.5} is otherwise fairly homogeneous across the Southeast US, reflecting
377 coherent stagnation, mixing, and ventilation of the region (X. Zhang et al., 2012; Pfister et al.,
378 2015). Sulfate accounts on average for 25% of PM_{2.5} while OA accounts for 55%. GEOS-Chem

Patrick 8/27/2015 11:44 AM

Deleted: to

380 captures the broad features shown in the surface station $PM_{2.5}$ data with little bias ($R = 0.65$,
381 normalized mean bias or NMB = -1.4%). The model hotspot in southern Arkansas is due to OA
382 from a combination of biogenic emissions and agricultural fires. As discussed below, agricultural
383 fires make only a small contribution on a regional scale.

384 The spatial distributions of sulfate and OC concentrations are shown in Figure 4. The
385 observed and simulated sulfate maxima are shifted to the northeast relative to total $PM_{2.5}$ shown
386 in Figure 3. GEOS-Chem captures a larger fraction of the observed variability at rural sites ($R =$
387 0.78 for IMPROVE) than at urban/suburban sites ($R = 0.71$ for SEARCH, 0.62 for CSN) as
388 would be expected from the sub-grid scale of urban pollution. A scatterplot of the simulated daily
389 mean surface sulfate concentrations compared to the filter observations from all three networks in
390 August-September 2013 is shown in the Supplementary Material. The model bias (NMB) is +5%
391 relative to IMPROVE, +10% relative to SEARCH, and +9% relative to CSN. Over the Southeast
392 US domain defined in Figure 2, 42% of sulfate production is from in-cloud production by H_2O_2 ,
393 22% is from gas-phase oxidation by OH, and 36% is from gas-phase oxidation by SCIs. Previous
394 studies by Pierce et al. (2013) and Boy et al. (2013) found similarly large contributions of SCIs to
395 sulfate production over forested regions in summer. However, there is substantial uncertainty in
396 the SCI kinetics, as discussed above, and it is possible that other oxidants are responsible for the
397 missing sulfate (hence the “Other” label in Figure 4).

398 The observed OC distribution shows a decreasing gradient from southwest to northeast
399 that maps onto the distribution of isoprene emissions shown in Figure 2. The IMPROVE OC is
400 generally low compared to CSN and SEARCH, as has been noted previously (Ford and Heald,
401 2013; Attwood et al., 2014). GEOS-Chem reproduces the broad features of the observed OC
402 distribution with moderate skill in capturing the variability ($R = 0.64$ for IMPROVE, 0.62 for
403 SEARCH, 0.61 for CSN). Model OC is biased high with a NMB of +66% for IMPROVE, +29%
404 for SEARCH, and +14% for CSN. The range of NMBs for the different networks could reflect
405 differences in measurement protocols described above - IMPROVE OC is lower than SEARCH
406 by 27% for collocated measurements made at Birmingham, Alabama (Supplementary Material).
407 We discuss this further in the next section in the context of the aircraft data.

408 Source attribution of OC in the model (Figure 4) suggests a dominance of biogenic
409 sources. Isoprene alone contributes 42% of the regional OC burden. This is in contrast with
410 previous work by Barsanti et al. (2013), who fitted chamber observations to a model mechanism
411 and found monoterpenes to be as or more important than isoprene as a source of OC in the
412 Southeast US (particularly under low-NO conditions). SEAC⁴RS observations support a

Patrick 8/27/2015 11:44 AM

Deleted:

414 | significant role of isoprene as a source of OA (W. Hu et al., 2015; Campuzano-Jost et al., 2015;
415 | Liao et al., 2015).

416 | Anthropogenic sources in the model contribute 28% to regional OC, roughly evenly
417 | distributed across the region. Open fires contribute 11%, mainly from agricultural fires in
418 | Arkansas and Missouri. Influence from western US fires is significant in the free troposphere (see
419 | Section 4) but not at the surface.

420 | When all of the components are taken together, we find that 81% of the surface OC in the
421 | Southeast US is secondary in origin. This is well above the 30-69% range of previous literature
422 | estimates for the region (Lim and Turpin, 2002; S. Yu et al., 2004; Kleindienst et al., 2007;
423 | Blanchard et al., 2008) and likely reflects the decreasing trend in anthropogenic emissions (Figure
424 | 1) and possibly a low bias in some estimation methods (Docherty et al., 2008). Assuming fossil
425 | fractions of 50% and 70% for anthropogenic primary and secondary OC respectively (Zotter et
426 | al., 2014; Hayes et al. 2014), we estimate that 18% of the total OC burden is derived from fossil
427 | fuel use. This is consistent with an 18% fossil fraction from radiocarbon measurements made on
428 | filter samples collected in Alabama during SOAS (Edgerton et al., 2014).

429 | 430 | **4. Aerosol Vertical Profile** 431 |

432 | We now examine the aerosol vertical distribution measured by the NASA DC-8 aircraft
433 | and simulated by GEOS-Chem along the flight tracks on 18 flights over the Southeast US (Figure
434 | 2). Aerosol mass composition was measured by a High-Resolution Aerodyne AMS for SNA and
435 | OA (Canagaratna et al., 2007) and by the NOAA humidified dual single-particle soot photometer
436 | for BC (HD-SP2; Schwarz et al., 2015). Dust concentrations were measured from filter samples
437 | (Dibb et al., 2003), but the ML values are ~10× higher than measured by surface networks or
438 | simulated in GEOS-Chem, as previously found by Drury et al. (2010) during ICARTT. Instead
439 | we estimate dust concentrations from Particle Analysis by Laser Mass Spectrometer (PALMS)
440 | measurements (Thomson et al., 2000; Murphy et al., 2006). The PALMS data provide the size-
441 | resolved number fraction of dust-containing particles, which is multiplied by the measured
442 | aerosol volume size distribution from the LAS instrument (Thornhill et al., 2008; Chen et al.,
443 | 2011) and an assumed density of 2.5 g cm⁻³. The size distribution is truncated to PM_{2.5} by
444 | applying the transmission curve for the 2.5 μm aerosol impactor used by the ground networks.

445 | Figure 5 shows the median sulfate, OA, and dust vertical profiles over the Southeast US.
446 | Also shown are the median concentrations from the surface networks over the study domain
447 | shown in Figure 2. The difference between the surface and aircraft data that can be attributed to

Patrick 8/27/2015 11:44 AM

Deleted: IEPOX-SOA (SOA formed from

Patrick 8/27/2015 11:44 AM

Deleted: by the main low-NO pathway) suggest that if anything the model underestimates the SOA yield from isoprene

Patrick 8/27/2015 11:44 AM

Deleted: was

Patrick 8/27/2015 11:44 AM

Deleted: can be inferred

454 differences in sampling (time and duration) is quantified by the difference in GEOS-Chem output
455 when the model is sampled with the surface data vs. when the model is sampled with the aircraft
456 data. For sulfate, the model underestimates the aircraft observations by 20% below 5 km but
457 overestimates the surface observations by 5-10% as discussed in Section 3. The general shape of
458 the vertical profile is well simulated (with a low bias from 3 to 4 km) and this applies also to SO₂
459 and to the SO₂/sulfate ratio (Supplementary Material). The sulfate concentrations are highest near
460 the surface and drop rapidly with altitude, but there is significant mass loading in the lower free
461 troposphere. 23% of the observed sulfate column mass lies in the free troposphere above 3 km
462 and this is well simulated by the model (23%). Analysis of SENEX and SEAC⁴RS vertical
463 profiles by Wagner et al. (2015) suggests that most of this free tropospheric sulfate is ventilated
464 from the PBL rather than being produced within the free troposphere from ventilated SO₂. GEOS-
465 Chem shows moderate skill in explaining the variability in the aircraft sulfate data (R = 0.81 for
466 all observations in the Southeast US, R = 0.68 below 3 km, R = 0.49 above 3 km).

467 Similarly to sulfate, OA measured from aircraft peaks at the surface and decreases rapidly
468 with height (Figure 5). The aircraft OA mass concentration below 1 km is 25-50% higher than
469 measured at the surface networks. IMPROVE is substantially lower than the other networks, as
470 has been noted above and in previous studies (Ford and Heald, 2013; Attwood et al., 2014), and
471 may be due to instrumental issues particular to that network. The discrepancy between the AMS
472 observations and CSN/SEARCH can largely be explained by differences in sampling, as shown
473 by the model. The GEOS-Chem simulation matches closely the aircraft observations. The vertical
474 distribution of OA is similar to that of sulfate, with 20% of the total column being above 3 km
475 both in the model and in the observations. The GEOS-Chem source attribution, also shown in
476 Figure 5, indicates that open fires contribute ~50% of OA in the free troposphere. This fire
477 influence is seen in the observations as occasional plumes of OA up to 6-7 km altitude (individual
478 gray dots in Figure 5). Fire plumes can be problematic for interpreting the AOD/PM relationship
479 for individual scenes but much less so in a temporal average as the mean influence on the column
480 is small. Simulating fire influence successfully in the model does require buoyant injection of
481 western US wildfire emissions in the free troposphere, as noted in previous studies (Turquety et
482 al., 2007; Fischer et al., 2014).

483 Comparison of GEOS-Chem to the individual OA observations along the aircraft flight
484 tracks shows good simulation of the variability (R = 0.82 for all observations, R = 0.74 below 3
485 km, R = 0.42 above 3 km). This is despite (or maybe because of) our use of a very simple
486 parameterization for the OA source. [Further GEOS-Chem comparison to SEAC⁴RS and SOAS
487 observations is presented by Marais et al. \(2015\) using a more mechanistic analysis of SOA.](#) The

Patrick 8/27/2015 11:44 AM

Deleted: ; these small inconsistent biases may not be significant.

Patrick 8/27/2015 11:44 AM

Deleted: while being 14-66% higher than the surface networks as reported above

492 successful GEOS-Chem simulation of the OA vertical profile argues against a large CCL source
493 from aqueous-phase cloud processing. This is supported by the work of Wagner et al. (2015),
494 who found little OA enhancement in air masses processed by cumulus wet convection.

495 Dust made only a minor contribution to total aerosol mass in the Southeast US during
496 SEAC⁴RS, accounting for less than 10% of observed surface PM_{2.5} (Figure 3). The PBL dust
497 concentrations measured by PALMS are roughly consistent with the surface data but the model is
498 much lower (Figure 5). This reflects a southward bias in the model transport of Saharan dust
499 (Fairlie et al., 2007), but is of little consequence for the simulation of PM_{2.5} or the AOD/PM
500 relationship over the Southeast US. Figure 5 shows few free tropospheric plumes in the
501 SEAC⁴RS observations, consistent with the dust climatology compiled from CALIOP data by D.
502 Liu et al. (2008).

503 Figure 6 compiles the median observed and simulated vertical profiles of aerosol
504 concentrations and composition during SEAC⁴RS. OA and sulfate dominate at all altitudes.
505 Ammonium is associated with sulfate as discussed in the next Section. OA accounts for most of
506 PM_{2.5} below 1 km, with a mass fraction $F_{OA} = [OA]/[PM_{2.5}]$ of 0.62 g g⁻¹ (0.65 in GEOS-Chem).
507 This is consistent with the surface SEARCH data ($F_{OA} = 0.56$ g g⁻¹). Figure 1 shows a lower F_{OA}
508 in the IMPROVE surface observations, increasing from 0.34 g g⁻¹ in 2003 to 0.44 g g⁻¹ in 2013,
509 reflecting instrumentation bias as discussed above. The aircraft data show that most of the aerosol
510 mass is OA at all altitudes. The aerosol column is mostly in the PBL (60% in the ML, ~25% in
511 the CCL), but ~15% is in the free troposphere with 10% above 5 km (Figure 6, right panel).
512 GEOS-Chem reproduces the observed shape of the vertical distribution of total aerosol mass, and
513 this is an important result for application of the model to derive the AOD/PM relationship.

514

515 5. Extent of Neutralization of Sulfate Aerosol

516

517 The extent of neutralization of sulfate aerosol by ammonia, computed from the fraction f
518 $= [NH_4^+]/(2[SO_4^{2-}] + [NO_3^-])$ where concentrations are molar, has important implications for the
519 aerosol phase and hygroscopicity, for the formation of aerosol nitrate (S. Martin et al., 2004; J.
520 Wang et al., 2008), and for the formation of SOA (Froyd et al., 2010; Eddingsaas, et al., 2012;
521 McNeill et al., 2012; Budisulistiorini et al., 2013; Liao et al., 2015). Figure 6 shows ammonium
522 to be the third most important aerosol component by mass in the Southeast US in summer after
523 OA and sulfate. Summertime particle-phase ammonium concentrations have declined at
524 approximately the same rate as sulfate from 2003 to 2013 (Figure 1 and Blanchard et al., 2013).
525 However, we find no significant trend over that time in ammonium wet deposition fluxes over the

Patrick 8/27/2015 11:44 AM

Deleted:

Patrick 8/27/2015 11:44 AM

Deleted: 66

Patrick 8/27/2015 11:44 AM

Deleted: 20

Patrick 8/27/2015 11:44 AM

Deleted: 20

Patrick 8/27/2015 11:44 AM

Deleted: closely

531 Southeast US (National Atmospheric Deposition Program, 2015), in contrast to a ~50% decline in
532 sulfate wet deposition. This implies that ammonia emissions have not decreased but the
533 partitioning into the aerosol has.

534 One would expect ammonium aerosol trends to follow those of sulfate if the aerosol is
535 fully neutralized ($f = 1$), so that partitioning of ammonia into the aerosol phase is limited by the
536 supply of sulfate. However, this is not the case in the observations. Figure 7 shows the extent of
537 neutralization in the observations and the model assuming that the SNA aerosol is externally
538 mixed from other ionic aerosol components such as dust. The model aerosol is fully neutralized
539 ($f = 1$) but the observed aerosol is not, with a median extent of neutralization of $0.55 \text{ mol mol}^{-1}$ in
540 the CSN data and $0.68 \text{ mol mol}^{-1}$ in the AMS data below 2 km. This is comparable to $f = 0.49$
541 mol mol^{-1} observed at the SOAS Centreville site earlier in the summer. The CSN data include full
542 ionic analysis and we examined whether internal mixing of SNA aerosol with other ions could
543 affect the extent of neutralization. The top right panel of Figure 7 shows that it does not,
544 reflecting the low concentrations of these other ions. The AMS reports total sulfate. While
545 organosulfates have a low pK_a and would interact with ammonium as a single charged ion, they
546 were typically a small fraction of total sulfate (Liao et al., 2015).

547 A possible explanation is that ammonia uptake by aerosol with $f < 1$ may be inhibited by
548 organic particle material. This has been demonstrated in a laboratory study by Liggio et al.
549 (2011), who show that the time constant for ammonia to be taken up by sulfate aerosol with
550 incomplete extent of neutralization increases with the ratio of condensing organic gases to sulfate
551 and may be hours to days. ▽

552 The complete extent of neutralization of sulfate aerosol in the model, in contrast to the
553 observations, leads to bias in the simulated aerosol phase and hygroscopicity for relating AOD to
554 PM. Calculations by J. Wang et al. (2008) for ammonium-sulfate particles of different
555 compositions show a 10-20% sensitivity of the mass extinction efficiency to the extent of
556 neutralization, with the effect changing sign depending on composition and RH. An additional
557 effect of $f = 1$ in the model would be to allow formation of ammonium nitrate aerosol, but nitrate
558 aerosol is negligibly small in the model as it is in the observations (Figure 6). At the high
559 temperatures over the Southeast US in the summer, we find in the model that the product of
560 HNO_3 and NH_3 partial pressures is generally below the equilibrium constant for formation of
561 nitrate aerosol. By contrast, surface network observations in winter show nitrate to be a large
562 component of surface $\text{PM}_{2.5}$ (Figure 1; Hand et al., 2012b; Ford and Heald, 2013), reflecting both
563 lower temperatures and the lower levels of sulfate.

564

Patrick 8/27/2015 11:44 AM

Deleted: We tested this hypothesis by examining the relationship between the model neutralization bias (the difference between simulated and observed f) and the OA concentration in the aircraft observations below 1 km, assuming sulfate and OA to be internally mixed (consistent with the PALMS observations). We find a significant correlation ($R = -0.33$, with a bootstrapped 95% confidence interval of $[-0.40, -0.25]$) as shown in Figure 8, which provides some support for organic-driven inhibition of ammonia uptake by sulfate aerosol.

576 6. Aerosol Extinction and Optical Depth

577

578 We turn next to light extinction measurements onboard the DC-8 to better understand the
579 relationship between the vertical profiles of aerosol mass (Section 4) and AOD. Aerosol
580 extinction coefficients were measured on the SEAC⁴RS aircraft remotely above and below the
581 aircraft by the NASA HSRL and at the altitude of the aircraft by the in situ NOAA cavity
582 ringdown spectrometer (CRDS; Langridge et al., 2011). Figure 8 compares the two
583 measurements, both at 532 nm, with GEOS-Chem. Though the two instruments sampled different
584 regions of the atmosphere at any given time, the mission median profiles are similar. The
585 exception is between 2 and 4 km where the HSRL extinction coefficient is lower. The shapes of
586 the vertical extinction profiles are consistent with aerosol mass (Figure 6). The fraction of total
587 column aerosol extinction below 3 km is 93% for the HSRL data (91% in GEOS-Chem when
588 sampled at the observation times) and 85% for the CRDS data (85% in GEOS-Chem). Almost all
589 of the column extinction is below 5 km (94% for the CRDS and 93% for GEOS-Chem).
590 Integrated up to the ceiling of the DC-8 aircraft, the median AODs from HSRL and the CRDS are
591 0.14 and 0.17 respectively (0.12 and 0.15 for GEOS-Chem).

592 Figure 9 shows maps of the mean AOD over the Southeast US in August-September
593 2013 as measured by AERONET, MISR, MODIS on the Aqua satellite, and simulated by GEOS-
594 Chem. The model is sampled at the local satellite overpass times (1030 for MISR and 1330 for
595 MODIS). We use the Version 31 Level 3 product from MISR (gridded averages at 0.5° x 0.5°
596 resolution) and the Collection 6 Level 3 product from MODIS (gridded averages at 1° x 1°
597 resolution). We exclude MODIS observations with cloud fraction greater than 0.5 or AOD greater
598 than 1.5 to account for cloud contamination and sensor saturation as in Ford and Heald (2013).
599 We use the Level 2 cloud-filtered daytime average AERONET observations, which can be
600 viewed as a reference measurement.

601 Comparison of daily collocated MODIS and MISR retrievals with AERONET
602 observations shows high correlation and little bias (statistics inset in Figure 9). These statistics
603 were calculated only when there are collocated and corresponding data for both AERONET and
604 the satellite retrieval, whereas Figure 9 shows the spatial average of all available data during
605 August-September 2013. MODIS shows a broad maximum over the Southeast US that
606 corresponds well with observed PM_{2.5} in Figure 3. There is greater heterogeneity in the MISR
607 average due to sparse sampling. GEOS-Chem captures the spatial pattern of the regional AOD
608 enhancement when sampled with the different retrievals and underestimates the magnitude by
609 16% (NMB relative to AERONET), consistent with the underestimate of the aircraft aerosol

Patrick 8/27/2015 11:44 AM

Deleted: 9

Patrick 8/27/2015 11:44 AM

Deleted: The atmosphere below 3 km contributes more to total aerosol extinction than to aerosol mass (80%, see Section 4) because of higher RH and hence hygroscopic growth of particles.

Patrick 8/27/2015 11:44 AM

Deleted: 10

Patrick 8/27/2015 11:44 AM

Deleted: 10).

Patrick 8/27/2015 11:44 AM

Formatted: Font:12 pt, Font color: Red

617 extinction data (including the NASA Ames 4STAR sun photometer, Supplementary Material).
618 The model underestimates AOD (NMB) by 28% relative to MODIS and by 8% relative to MISR.

Patrick 8/27/2015 11:44 AM

Deleted: .

620 7. The Aerosol Seasonal Cycle

621

622 As pointed out in the introduction, there has been considerable interest in interpreting the
623 aerosol seasonal cycle over the Southeast US and the difference in seasonal amplitude between
624 AOD and surface PM_{2.5} (Goldstein et al. 2009, Ford and Heald, 2013). Figure 10 shows MODIS
625 monthly average AOD over the Southeast US for 2006-2013. The observed AOD in 2013 shows
626 a seasonal cycle consistent with previous years. There has been a general decline in the seasonal
627 amplitude over 2006-2013 driven by a negative summertime trend, with 2011 being anomalous
628 due to high fire activity. The same long-term decrease and 2011 anomaly are seen in the surface
629 PM_{2.5} data (Figure 1). Examination of Figure 10 reveals that the entirety of the seasonal decrease
630 from summer to winter takes place as a sharp transition in the August-October window, in all
631 years.

Patrick 8/27/2015 11:44 AM

Deleted: 11

Patrick 8/27/2015 11:44 AM

Deleted: (NOAA, 2011).

Patrick 8/27/2015 11:44 AM

Deleted: 11

632 We analyzed the causes of this August-October transition using the GEOS-Chem
633 simulation of the SEAC⁴RS period. Figure 11 (panel A) shows the time series of daily median
634 AOD from AERONET, GEOS-Chem sampled at the times and locations of the AERONET
635 observations, and MODIS over the Southeast US. The difference between AERONET and
636 MODIS can be explained by differences in sampling (they otherwise correspond well with each
637 other, see Section 6). Observations through early September show large oscillations with a 7-10
638 day period driven by frontal passages. These are well reproduced by the model. The observed
639 AODs then fall sharply in mid-September and again this is well reproduced by GEOS-Chem. The
640 successful simulation of the August-October seasonal transition implies that we can use the
641 model to understand the causes of this transition. Figure 11 also shows the sulfate and OA
642 contributions to GEOS-Chem AOD. Sulfate aerosol contributes as much to column light
643 extinction as OA, despite lower concentrations, due to its higher mass extinction efficiency. Both
644 the sulfate and OA contributions to AOD fall during the seasonal transition.

Patrick 8/27/2015 11:44 AM

Deleted: 12

645 We find that the sharp drops in sulfate and OA concentrations over August-October are
646 due to two factors. The first is a decline in isoprene and monoterpene emissions due to cooler
647 surface temperatures and leaf senescence (panel B of Figure 11). The second is a transition in the
648 photochemical regime as UV radiation sharply declines (Kleinman, 1991; Jacob et al., 1995),
649 depleting OH and H₂O₂ (panel C) and hence sulfate formation.

Patrick 8/27/2015 11:44 AM

Deleted: 12

Patrick 8/27/2015 11:44 AM

Deleted: 12

657 The seasonal transition in photochemical regime also involves a shift from a low-NO to a
658 high-NO chemical regime (Kleinman, 1991; Jacob et al., 1995). This would affect the SOA yield
659 (Marais et al., 2015), though this is not represented in the current GEOS-Chem simulation. Panel
660 D of Figure [11](#) shows the ratio of isoprene hydroperoxides (ISOPOOH) to isoprene nitrate
661 (ISOPN) concentrations measured in the PBL during SEAC⁴RS by the Caltech CIMS (Crouse et
662 al., 2006; St. Clair et al., 2010) and simulated by GEOS-Chem. ISOPOOH is formed under low-
663 NO conditions, while ISOPN is formed under high-NO conditions. Both observations and the
664 model show a decline in the ISOPOOH/ISOPN concentration ratio over the course of SEAC⁴RS,
665 with the model showing extended decline into October. If the SOA yield is higher under low-NO
666 conditions (Kroll et al., 2005, 2006; Xu et al. 2014) then this would also contribute to the
667 seasonal decline in OA.

668 We have thus explained the seasonality of AOD as driven by aerosol sources. Previous
669 studies have pointed out that surface PM_{2.5} in the Southeast US has much weaker seasonality than
670 AOD, and observed PM_{2.5} in 2013 had no significant seasonality (Figure [12](#), top panel). This
671 difference in the amplitude of the seasonal cycle between PM_{2.5} and AOD is also simulated by
672 GEOS-Chem, as shown in Figure [12](#). It is driven in GEOS-Chem by the seasonal variation in ML
673 height (middle panel of Figure [12](#)), dampening the seasonal cycle of PM_{2.5} by reducing
674 ventilation in winter. The AOD in GEOS-Chem is lower than observed in summer and higher in
675 winter, so that the seasonality is weaker than observed, (a factor of 2 compared to an observed
676 factor of 3-4). The summer underestimate is consistent with the aircraft observations, as discussed
677 previously. The winter overestimate could reflect seasonal error in model aerosol sources or
678 optical properties.

679 8. Conclusions

681
682 We have used a large ensemble of surface, aircraft, and satellite observations during the
683 SEAC⁴RS field campaign over the Southeast US in August-September 2013 to better understand
684 (1) the sources of sulfate and organic aerosol (OA) in the region; (2) the relationship between the
685 aerosol optical depth (AOD) measured from space and the fine particulate matter concentration
686 (PM_{2.5}) measured at the surface; and (3) the seasonal aerosol cycle and the apparent inconsistency
687 between satellite and surface measurements. Our work used the GEOS-Chem global chemical
688 transport model (CTM) with 0.25° x 0.3125° (~25 x 25 km²) horizontal resolution over North
689 America as an integrative platform to compare and interpret the ensemble of observations.

690 PM_{2.5} surface observations are fairly homogenous across the Southeast US, reflecting

Patrick 8/27/2015 11:44 AM

Deleted: .

Patrick 8/27/2015 11:44 AM

Deleted: 12

Patrick 8/27/2015 11:44 AM

Deleted: 13

Patrick 8/27/2015 11:44 AM

Deleted: 13

Patrick 8/27/2015 11:44 AM

Deleted: 13

Patrick 8/27/2015 11:44 AM

Deleted: .

697 regional coherence in stagnation, mixing, and ventilation. Sulfate and OA account for the bulk of
698 PM_{2.5}. GEOS-Chem simulates sulfate without bias but this requires uncertain consideration of
699 SO₂ oxidation by stabilized Criegee intermediates to account for 30% of sulfate production. The
700 OA simulation bias is +14% relative to CSN sites and +66% relative to IMPROVE sites but the
701 IMPROVE data may be too low. OA in the model originates from biogenic isoprene (40%) and
702 monoterpenes (20%), anthropogenic sources (30%) and open fires (10%).

703 Aircraft vertical profiles show that 60% of the aerosol column mass is in the mixed layer
704 (ML), 25% is in the convective cloud layer (CCL), and 15% is in the free troposphere (FT). This
705 is well reproduced in GEOS-Chem. OA accounts for 65% of the aerosol column mass in the
706 observations and in the model. The successful simulation of OA vertical profiles argues against a
707 large OA source in the free troposphere other than PBL ventilation. Occasional fire and dust
708 plumes were observed in the free troposphere but have little impact on temporal averages.

709 The extent of neutralization of sulfate aerosol over the Southeast US ($f = [\text{NH}_4^+]/(2[\text{SO}_4^{2-}]$
710 $+ [\text{NO}_3^-])$) is observed to be in the range 0.49-0.68 mol mol⁻¹ for the different data sets, despite an
711 excess of ammonia being present. This is inconsistent with thermodynamic equilibrium and with
712 the observation of a 2003-2013 decline in ammonium aerosol concentrations paralleling that of
713 sulfate. We hypothesize that the departure from equilibrium is correlated with OA, as supported
714 by laboratory findings by Liggio et al. (2011) that organic particle material may impede ammonia
715 uptake by sulfate aerosol. This may have important implications for aerosol hygroscopicity and
716 chemistry.

717 The vertical profile of aerosol light extinction measured from the aircraft follows closely
718 that of aerosol mass. GEOS-Chem has a ~16% low bias in aerosol extinction compared to these
719 observations and simulates correctly the vertical profile. Sulfate accounts for as much of the
720 column light extinction as OA, despite lower mass concentrations. Evaluation of collocated
721 MODIS and MISR AOD retrievals with AERONET shows excellent agreement. GEOS-Chem is
722 16% too low compared to AERONET and 7-28% too low compared to MODIS and MISR,
723 consistent with its bias relative to the aircraft extinction data. We thus find reasonable agreement
724 between AODs measured from space and from the surface, aircraft aerosol extinction and mass
725 profiles, and surface PM_{2.5} measurements, the largest discrepancy being between different
726 measurements of OA.

727 We find that the previously reported summer-to-winter decrease in MODIS AOD data
728 over the Southeast US is driven by a sharp August-to-October transition, in all years. This
729 seasonal transition is well captured by GEOS-Chem where it is caused by declines in both sulfate
730 and OA. Biogenic emissions of isoprene and monoterpenes shut down during this time period due

Patrick 8/27/2015 11:44 AM

Deleted: 20

Patrick 8/27/2015 11:44 AM

Deleted: 20

Patrick 8/27/2015 11:44 AM

Deleted: find

Patrick 8/27/2015 11:44 AM

Deleted: in the aircraft observations, supporting

Patrick 8/27/2015 11:44 AM

Deleted: The aerosol above the PBL accounts for 15% of column light extinction, versus 20% of column mass, reflecting the lower RH at higher altitudes.

Patrick 8/27/2015 11:44 AM

Deleted: excellent closure

740 to lower temperatures and leaf senescence, and rapidly declining UV radiation suppresses SO₂
741 oxidation by OH and H₂O₂. The seasonal decline of UV radiation also suppresses the low-NO
742 pathway of isoprene oxidation, which may be associated with larger OA yields than the high-NO
743 pathway.

744 Previous studies have pointed out an apparent inconsistency between the large seasonal
745 variation of AOD measured from space and the much weaker seasonal variation of PM_{2.5}
746 measured at the surface (Goldstein et al., 2009; Ford and Heald, 2013). We find that this can be
747 largely explained by the seasonal trend in boundary layer ventilation, offsetting the effect of
748 decreased wintertime PM sources on the surface concentrations. Overall our results show that
749 measured AODs from space are consistent with measurements of PM_{2.5} air quality in the
750 Southeast US. This implies that satellite measurements can reliably be used to infer PM_{2.5} if a
751 good CTM representation of PBL mixing and ventilation is available.

752
753
754
755
756
757
758
759
760
761
762
763
764
765
766
767
768
769
770
771
772
773

Patrick 8/27/2015 11:44 AM

Deleted: fundamentally

775 | **Acknowledgements**

776

777

778

779

780

781 |

782

783

784

785

786

787

788

789

790

791

792

793

794

795

796

797

798

799

800

801

802

803

804

805

806

807

808

We are grateful to the entire NASA SEAC⁴RS team for their help in the field. We thank Aaron van Donkelaar, Eloise Marais, Loretta Mickley, Randall Martin, Chuck Brock, Ann Dillner, Ralph Kahn, Armin Sorooshian, Tran Nguyen, and Jenny Hand for helpful discussions and Sajeev Philip for assistance with downloading meteorological fields. We also thank Jack Dibb, Bruce Anderson and the LARGE team, [Phil Russell](#), [Jens Redemann and the 4STAR team](#), and Greg Huey for the data shown in the Supplementary Material. This work was funded by the NASA Tropospheric Chemistry Program and by a Department of Energy Office of Science Graduate Fellowship to PSK made possible in part by the American Recovery and Reinvestment Act of 2009, administered by ORISE-ORAU under contract no. DE-AC05-06OR23100. PCJ and JLJ were supported by NASA NNX12AC03G and NSF AGS-1243354/1360834. KF and JL are supported by NASA grant NNH12AT29I from the Upper Atmosphere Research Program, Radiation Sciences Program, and Tropospheric Chemistry Program, and by NOAA base funding. DBM acknowledges support from NSF (Grant #1148951). POW, JDC, JMS, and APT acknowledge support from NASA (NNX12AC06G and NNX14AP46G). We thank the U.S. EPA for providing the 2010 North American emission inventory. The inventory is intended for research purposes and was developed for Phase 2 of the Air Quality Model Evaluation International Initiative (AQMEII) using information from the 2008-based modeling platform as a starting point. A technical document describing the 2008-based 2007v5 modeling platform can be found at epa.gov/ttn/chief/emch/2007v5/2007v5_2020base_EmisMod_TSD_13dec2012.pdf. A report on the 2008 NEI can be found at www.epa.gov/ttn/chief/net/2008report.pdf. GEOS-Chem is managed by the Harvard University Atmospheric Chemistry Modeling Group with support from the NASA Atmospheric Composition Modeling and Analysis Program. The GEOS-FP data used in this study were provided by the Global Modeling and Assimilation Office (GMAO) at NASA Goddard Space Flight Center.

Patrick 8/27/2015 11:44 AM

Deleted: -

... [1]

811 **References**

812

813 Alston, E. J., Sokolik, I. N., and Kalashnikova, O. V.: Characterization of atmospheric aerosol in
814 the US Southeast from ground- and space-based measurements over the past decade,
815 *Atmos. Meas. Tech.*, 5, 1667-1682, doi:10.5194/amt-5-1667-2012, 2012.

816 Attwood, A. R., Washenfelder, R. A., Brock, C. A., Hu, W., Baumann, K., Campuzano-Jost, P.,
817 Day, D. A., Edgerton, E. S., Murphy, D. M., Palm, B. B., McComiskey, A., Wagner, N.
818 L., de Sa, S. S., Ortega, A., Martin, S. T., Jimenez, J. L., and Brown, S. S.: Trends in
819 sulfate and organic aerosol mass in the Southeast U.S.: Impact on aerosol optical depth
820 and radiative forcing, *Geophys. Res. Lett.*, 41, 7701-7709, doi:10.1002/2014GL061669,
821 2014.

822 Baasandorj, M., Millet, D. B., Hu, H., Mitroo, D., and Williams, B. J.: Measuring acetic and
823 formic acid by proton-transfer-reaction mass spectrometry: sensitivity, humidity
824 dependence, and quantifying interferences, *Atmos. Meas. Tech.*, 8, 1303-1321,
825 doi:10.5194/amt-8-1303-2015, 2015.

826 Barsanti, K. C., Carlton, A. G., and Chung, S. H.: Analyzing experimental data and model
827 parameters: implications for predictions of SOA using chemical transport models, *Atmos.*
828 *Chem. Phys.*, 13, 12073-12088, doi:10.5194/acp-13-12073-2013, 2013

829 Blanchard, C. L., Hidy, G. M., Tanenbaum, S., Edgerton, E., Hartsell, B., and Jansen, J.: Carbon
830 in southeastern US aerosol particles: empirical estimates of secondary organic aerosol
831 formation, *Atmos. Environ.*, 42, 6710-6720, doi:10.1016/j.atmosenv.2008.04.011, 2008.

832 Blanchard, C. L., Hidy, G. M., Tanenbaum, S., Edgerton, E. S., and Hartsell, B. E.: The
833 Southeastern Aerosol Research and Characterization (SEARCH) study: Temporal trends
834 in gas and PM concentrations and composition, 1999-2010, *J. Air Waste Manage. Assoc.*,
835 63(3), 247-259, doi:10.1080/10962247.2012.748523, 2013.

836 Boy, M., Mogensen, D., Smolander, S., Zhou, L., Nieminen, T., Paasonen, P., Plass-Dulmer, C.,
837 Sipila, M., Petaja, T., Mauldin, L., Berresheim, H., and Kulmala, M.: Oxidation of SO₂
838 by stabilized Criegee Intermediate (sCI) radicals as a crucial source for atmospheric
839 sulfuric acid concentrations, *Atmos. Chem. Phys.*, 13, 3865-3879, doi:10.5194/acp-13-
840 3865-2013, 2013.

841 Boys, B. L., Martin, R. V., van Donkelaar, A., MacDonell, R. J., Hsu, N. C., Cooper, M. J.,
842 Yantosca, R. M., Lu, Z., Streets, D. G., Zhang, Q., and Wang, S. W.: Fifteen-year global
843 time series of satellite-derived fine particulate matter, *Environ. Sci. Technol.*, 48, 11109-
844 11118, doi:10.1021/es502113p, 2014.

845 Budisulistiorini, S. H., Canagaratna, M. R., Croteau, P. L., Marth, W. J., Baumann, K., Edgerton,
846 E. S., Shaw, S. L., Knipping, E. M., Worsnop, D. R., Jayne, J. T., Gold, A., and Surratt, J.
847 D.: Real-time continuous characterization of secondary organic aerosol derived from
848 isoprene epoxydiols in downtown Atlanta, Georgia, using the Aerodyne Chemical
849 Speciation Monitor, *Environ. Sci. Technol.*, 47, 5686-5694, doi:10.1021/es400023n,
850 2013.

851 Campuzano-Jost, P., Palm, B., Day, D., Hu, W., Ortega, A., Jimenez, J., Liao, J., Froyd, K.,
852 Pollack, I., Peischl, J., Ryerson, T., St. Clair, J., Crounse, J., Wennberg, P., Mikoviny, T.,
853 Wisthaler, A., Ziemba, L., and Anderson, B.: Secondary organic aerosol (SOA) derived
854 from isoprene epoxydiols: Insights into formation, aging, and distribution over the
855 continental US from the DC3 and SEAC4RS campaigns, Abstract A33M-02 presented at
856 2014 Fall Meeting, AGU, San Francisco, Calif., 15-19 Dec, 2014.

857 Canagaratna, M. R., Jayne, J. T., Jimenez, J. L., Allan, J. D., Alfarra, M. R., Zhang, Q., Onasch,
858 T. B., Drewnick, F., Coe, H., Middlebrook, A., Delia, A., Williams, L. R., Trimborn, A.
859 M., Northway, M. J., DeCarlo, P. F., Kolb, C. E., Davidovits, P., and Worsnop, D. R.:
860 Chemical and microphysical characterization of ambient aerosols with the aerodyne
861 aerosol mass spectrometer, *Mass Spectrometry Reviews*, 26(2), 185-222,
862 doi:10.1002/mas.20115, 2007.

863 Canagaratna, M. R., Jimenez, J. L., Kroll, J. H., Chen, Q., Kessler, S. H., Massoli, P., Hildebrandt
864 Ruiz, L., Fortner, E., Williams, L. R., Wilson, K. R., Surratt, J. D., Donahue, N. M.,
865 Jayne, J. T., and Worsnop, D. R.: Elemental ratio measurements of organic compounds
866 using aerosol mass spectrometry: characterization, improved calibration, and
867 implications, *Atmos. Chem. Phys.*, 15, 253-272, doi:10.5194/acp-15-253-2015, 2015.

868 Carlton, A. G., Pinder, R. W., Bhave, P. K., and Pouliot, G. A.: To what extent can biogenic SOA
869 be controlled?, *Environ. Sci. Technol.*, 44, 3376-3380, doi:10.1021/es903506b, 2010.

870 Chan, A. W. H., Chan, M. N., Surratt, J. D., Chhabra, P. S., Loza, C. L., Crounse, J. D., Yee, L.
871 D., Flagan, R. C., Wennberg, P. O., and Seinfeld, J. H.: Role of aldehyde chemistry and
872 NO_x concentrations in secondary organic aerosol formation, *Atmos. Chem. Phys.*, 10,
873 7169-7188, doi:10.5194/acp-10-7169-2010, 2010.

874 Chao, W., Hsieh, J.-T., Chang, C.-H., and Lin, J. J.: Direct kinetic measurement of the reaction of
875 the simplest Criegee intermediate with water vapor, *Science*, 347(6223), 751-754,
876 doi:10.1126/science.1261549, 2015.

877 Chen, G., Ziemba, L. D., Chu, D. A., Thornhill, K. L., Schuster, G. L., Winstead, E. L., Diskin,
878 G. S., Ferrarre, R. A., Burton, S. P., Ismail, S., Kooi, S. A., Omar, A. H., Slusher, D. L.,

879 Kleb, M. M., Reid, J. S., Twohy, C. H., Zhang, H., and Anderson, B. E.: Observations of
880 Saharan dust microphysical and optical properties from the Eastern Atlantic during
881 NAMMA airborne field campaign, *Atmos. Chem. Phys.*, 11, 723-740, doi:10.5194/acp-
882 11-723-2011, 2011.

883 Chin, M., and Jacob, D. J.: Anthropogenic and natural contributions to tropospheric sulfate: A
884 global model analysis, *J. Geophys. Res.*, 101(D13), 18691-18699,
885 doi:10.1029/96JD01222, 1996.

886 Chow, J. C., Watson, J. G., Chen, L.-W. A., Rice, J., and Frank, N. H.: Quantification of PM_{2.5}
887 organic carbon sampling artifacts in US networks, *Atmos. Chem. Phys.*, 10, 5223-5239,
888 doi:10.5194/acp-10-5223-2010, 2010.

889 Crawford, J. H., and Pickering, K. E.: DISCOVER-AQ: Advancing strategies for air quality
890 observations in the next decade, *Environmental Manager*, 4-7, 2014.

891 Crounse, J. D., McKinney, K. A., Kwan, A. J., and Wennberg, P. O.: Measurement of gas-phase
892 hydroperoxides by chemical ionization mass spectrometry, *Anal. Chem.*, 78, 6726-6732,
893 doi:10.1021/ac0604235, 2006.

894 Cubison, M. J., Ortega, A. M., Hayes, P. L., Farmer, D. K., Day, D., Lechner, M. J., Brune, W.
895 H., Apel, E., Diskin, G. S., Fisher, J. A., Fuelberg, H. E., Hecobian, A., Knapp, D. J.,
896 Mikoviny, T., Riemer, D., Sachse, G. W., Sessions, W., Weber, R. J., Weinheimer, A. J.,
897 Wisthaler, A., and Jimenez, J. L.: Effects of aging on organic aerosol from open biomass
898 burning smoke in aircraft and laboratory studies, *Atmos. Chem. Phys.*, 11, 12049-12064,
899 doi:10.5194/acp-11-12049-2011, 2011.

900 Darmenov, A., and da Silva, A.: The Quick Fire Emissions Dataset (QFED) – Documentation of
901 versions 2.1, 2.2, and 2.4, NASA Technical Report Series of Global Modeling and Data
902 Assimilation, NASA TM-2013-104606, 32, 183 pp, 2013.

903 de Gouw, J. A., and Jimenez, J. L.: Organic aerosols in the Earth's atmosphere, *Environ. Sci.*
904 *Technol.*, 43, 7614-7618, doi:10.1021/es9006004, 2009.

905 Dibb, J. E., Talbot, R. W., Scheuer, E. M., Seid, G., Avery, M. A., and Singh, H. B.: Aerosol
906 chemical composition in Asian continental outflow during the TRACE-P campaign:
907 comparison with PEM-West B, *J. Geophys. Res.*, 108, 8815, doi:10.1029/2002JD003111,
908 D21, 2003.

909 Dillner, A. M., Phuah, C. H., and Turner, J. R.: Effects of post-sampling conditions on ambient
910 carbon aerosol filter measurements, *Atmos. Environ.*, 43, 5937-5943,
911 doi:10.1016/j.atmosenv.2009.08.009, 2009.

912 Diner, D. J., Braswell, B. H., Davies, R., Gobron, N., Hu, J., Jin, Y., Kahn, R. A., Knyazikhin,
913 Loeb, N., Muller, J.-P., Nolin, A. W., Pinty, B., Schaaf, C. B., Seiz, G., and Stroeve, J.:
914 The value of multiangle measurements for retrieving structurally and radiatively
915 consistent properties of clouds, aerosols, and surfaces, *Remote Sens. Environ.*, 97, 495-
916 518, doi:10.1016/j.rse.2005.06.006, 2005.

917 Docherty, K. S., Stone, E. A., Ulbrich, I. M., DeCarlo, P. F., Snyder, D. C., Schauer, J. J., Peltier,
918 R. E., Weber, R. J., Murphy, S. M., Seinfeld, J. H., Grover, B. D., Eatough, D. J., and
919 Jimenez, J. L.: Apportionment of primary and secondary organic aerosols in Southern
920 California during the 2005 Study of Organic Aerosols in Riverside (SOAR-1), *Environ.*
921 *Sci. Technol.*, 42, 7655-7662, doi:10.1021/es8008166, 2008.

922 Donahue, N. M., Robinson, A. L., Stanier, C. O., and Pandis, S. N.: Coupled partitioning,
923 dilution, and chemical aging of semivolatile organics, *Environ. Sci. Technol.*, 40, 2635-
924 2643, doi:10.1021/es052297c, 2006.

925 Drury, E., Jacob, D. J., Spurr, R. J. D., Wang, J., Shinzuka, Y., Anderson, B. E., Clarke, A. D.,
926 Dibb, J., McNaughton, C., and Weber, R.: Synthesis of satellite (MODIS), aircraft
927 (ICARTT), and surface (IMPROVE, EPA-AQS, AERONET) aerosol observations over
928 eastern North America to improve MODIS aerosol retrievals and constrain surface
929 aerosol concentrations and sources, *J. Geophys. Res.*, 115, D14204,
930 doi:10.1029/2009JD012629, 2010.

931 Eddingsaas, N. C., VanderVelde, D. G., and Wennberg, P. O.: Kinetics and products of the acid-
932 catalyzed ring-opening of atmospherically relevant butyl epoxy alcohols, *J. Phys. Chem.*
933 *A*, 114, 8106-8113, doi:10.1021/jp103907c, 2010.

934 Edgerton, E. S., Hartsell, B. E., Saylor, R. D., Jansen, J. J., Hansen, D. A., and Hidy, G. M.: The
935 Southeastern Aerosol Research and Characterization Study: Part II. Filter-based
936 measurements of fine and coarse particulate matter mass and composition, *J. Air &*
937 *Waste Manage. Assoc.*, 52, 1527-1542, doi:10.1080/10473289.2005.10464744, 2005.

938 Edgerton, E. S., et al.: First look at ¹⁴C data during the Centreville, AL SOAS campaign,
939 presented at the SAS Data Workshop, Boulder, Co., 31 Mar. – 2 Apr, 2014.

940 EPA.: Particulate matter (PM_{2.5}) speciation guidance, Final draft, Edition 1, October 7, 1999. U.S.
941 Environmental Protection Agency, Monitoring and Quality Assurance Group, Emissions,
942 Monitoring, and Analysis Division, Office of Air Quality Planning and Standards,
943 Research Triangle Park, NC. [http://www.epa.gov/ttn/amtic/files/ambient/
944 pm25/spec/specfinl.pdf](http://www.epa.gov/ttn/amtic/files/ambient/pm25/spec/specfinl.pdf), 1999.

945 Ervens, B., Turpin, B. J., and Weber, R. J.: Secondary organic aerosol formation in cloud droplets

946 and aqueous particles (aqSOA): a review of laboratory, field and model studies, *Atmos.*
947 *Chem. Phys.*, 11, 11069-11102, doi:10.5194/acp-11-11069-2011, 2011.

948 Fairlie, T. D., Jacob, D. J., and Park, R. J.: The impact of transpacific transport of mineral dust in
949 the United States, *Atmos. Environ.*, 41, 1251-1266, doi:10.1016/j.atmosenv.2006.09.048,
950 2007.

951 Fischer, E. V., Jacob, D. J., Yantosca, R. M., Sulprizio, M. P., Millet, D. B., Mao, J., Paulot, F.,
952 Singh, H. B., Roiger, A., Ries, L., Talbot, R. W., Dzepina, K., and Pandey Deolal, S.:
953 Atmospheric peroxyacetyl nitrate (PAN): a global budget and source attribution, *Atmos.*
954 *Chem. Phys.*, 14, 2679-2698, doi:10.5194/acp-14-2679-2014, 2014.

955 Fisher, J. A., Jacob, D., Travis, K., Cohen, R., Fried, A., Hanisco, T., Mao, J., Wennberg, P.,
956 Crounse, J., St. Clair, J., Teng, A., Wisthaler, A., Mikoviny, T., Jimenez, J., Campuzano-
957 Jost, P., Kim, P., Marais, E., Paulot, F., Yu, K., Zhu, L., Yantosca, R., and Sulprizio, M.:
958 Isoprene nitrate chemistry in the Southeast US: Constraints from GEOS-Chem and
959 SEAC⁴RS, presented at the SEAC⁴RS Science Team Meeting, Pasadena, Calif., 28 Apr –
960 1 May, 2015.

961 Ford, B., and Heald, C. L., Aerosol loading in the Southeastern United States: reconciling surface
962 and satellite observations, *Atmos. Chem. Phys.*, 13, 9269-9283, doi:10.5194/acp-13-
963 9269-2013, 2013.

964 Fountoukis, C., and Nenes, A.: ISORROPIA II: a computationally efficient thermodynamic
965 equilibrium model for K^+ - Ca^{2+} - Mg^{2+} - NH_4^+ - Na^+ - SO_4^{2-} - NO_3^- - Cl^- - H_2O aerosols, *Atmos.*
966 *Chem. Phys.*, 7, 4639-4659, doi:10.5194/acp-7-4639-2007, 2007.

967 Froyd, K. D., Murphy, S. M., Murphy, D. M., de Gouw, J. A., Eddingsaas, N. C., and Wennberg
968 P. O.: Contribution of isoprene-derived organosulfates to free tropospheric aerosol mass,
969 *Proc. Natl. Acad. Sci.*, 107(50), 21360-21365, doi:10.1073/pnas.1012561107, 2010.

970 Fu, T. M., Jacob, D. J., and Heald, C. L.: Aqueous-phase reactive uptake of dicarbonyls as a
971 source of organic aerosol over eastern North America, *Atmos. Environ.*, 43, 1814-1822,
972 doi: 10.1016/j.atmosenv.2008.12.029, 2009.

973 Goldstein, A. H., Koven, C. D., Heald, C. L., and Fung, I. Y.: Biogenic carbon and anthropogenic
974 pollutants combine to form a cooling haze over the southeastern United States, *Proc.*
975 *Natl. Acad. Sci.*, 106(22), 8835-8840, doi:10.1073/pnas.0904128106, 2009.

976 Guenther, A. B., Jiang, X., Heald, C. L., Sakulyanontvittaya, T., Duhl, T., Emmons, L. K., and
977 Wang, X.: The Model of Emissions of Gases and Aerosols from Nature version 2.1
978 (MEGAN2.1): an extended and updated framework for modeling biogenic emissions,
979 *Geosci. Model Dev.*, 5, 1471-1492, doi:10.5194/gmd-5-1471-2012, 2012.

980 Hair, J. W., Hostetler, C. A., Cook, A. L., Harper, D. B., Ferrare, R. A., Mack, T. L., Welch, W.,
981 Izquierdo, L. R., and Hovis, F. E.: Airborne High Spectral Resolution Lidar for profiling
982 aerosol optical properties, *Appl. Optics*, 47, 6734-6752, doi:10.1364/AO.47.006734,
983 2008.

984 Hand, J. L., Schichtel, B. A., Pitchford, M., Malm, W. C., and Frank, N. H.: Seasonal
985 composition of remote and urban fine particulate matter in the United States, *J. Geophys.*
986 *Res.*, 117, D05209, doi:10.1029/2011JD017122, 2012a.

987 Hand, J. L., Schichtel, B. A., Malm, W. C., and Pitchford, M. L.: Particulate sulfate ion
988 concentration and SO₂ emission trends in the United States from the early 1990s through
989 2010, *Atmos. Chem. Phys.*, 12, 10353-10365, doi:10.5194/acp-12-10353-2012, 2012b.

990 Hayes, P. L., Carlton, A. G., Baker, K. R., Ahmadov, R., Washenfelder, R. A., Alvarez, S.
991 Rappengluck, B., Gilman, J. B., Kuster, W. C., de Gouw, J. A., Zotter, P., Prevot, A. S.
992 H., Szidat, S., Kleindienst, T. E., Offenberg, J. H., and Jimenez, J. L.: Modeling the
993 formation and aging of secondary organic aerosols in Los Angeles during CalNex 2010,
994 *Atmos. Chem. Phys. Discuss*, 14, 32325-32391, doi:10.5194/acpd-14-32325-2014, 2014.

995 Heald, C. L., Jacob, D. J., Turquety, S., Hudman, R. C., Weber, R. J., Sullivan, A. P., Peltier, R.
996 E., Atlas, E. L., de Gouw, J. A., Warneke, C., Holloway, J. S., Neuman, J. A., Flocke, F.
997 M., and Seinfeld, J. H.: Concentrations and sources of organic carbon aerosols in the free
998 troposphere over North America, *J. Geophys. Res.*, 111, D23S47,
999 doi:10.1029/2006JD007705, 2006a.

1000 Heald, C. L., Jacob, D. J., Park, R. J., Alexander, B., Fairlie, T. D., Yantosca, R. M., and Chu, D.
1001 A.: Transpacific transport of Asian anthropogenic aerosols and its impact on surface air
1002 quality in the United States, *J. Geophys. Res.*, 111, D14310, doi:10.1029/2005JD006847,
1003 2006b.

1004 Heald, C. L., Coe, H., Jimenez, J. L., Weber, R. J., Bahreini, R., Middlebrook, A. M., Russell, L.
1005 M., Jolleys, M., Fu, T.-M., Allan, J. D., Bower, K. N., Capes, G., Crosier, J., Morgan, W.
1006 T., Robinson, N. H., Williams, P. I., Cubison, M. J., DeCarlo, P. F., and Dunlea, E. J.:
1007 Exploring the vertical profile of atmospheric organic aerosol: comparing 17 aircraft field
1008 campaigns with a global model, *Atmos. Chem. Phys.*, 11, 12673-12696, doi:10.5194/acp-
1009 11-12673-2011, 2011.

1010 Heald, C. L., Collett Jr., J. L., Lee, T., Benedict, K. B., Schwandner, F. M., Li, Y., Clarisse, L.,
1011 Hurtmans, D. R., Van Damme, M., Clerbaux, C., Coheur, P.-F., Philip, S., Martin, R. V.,
1012 and Pye, H. O. T.: Atmospheric ammonia and particulate inorganic nitrogen over the

1013 United States, *Atmos. Chem. Phys.*, 12, 10295-10312, doi:10.5194/acp-12-10295-2012,
1014 2012.

1015 Henze, D. K., and Seinfeld, J. H.: Global secondary organic aerosol from isoprene oxidation,
1016 *Geophys. Res. Lett.*, 33, L09812, doi:10.1029/2006GL025976, 2006.

1017 Hermansson, E., Roldin, P., Rusanen, A., Mogensen, D., Kivekas, N., Vaananen, R., Boy, M.,
1018 and Swietlicki, E.: Biogenic SOA formation through gas-phase oxidation and gas-to-
1019 particle partitioning – a comparison between process models of varying complexity,
1020 *Atmos. Chem. Phys.*, 14, 11853-11869, doi:10.5194/acp-14-11853-2014, 2014.

1021 Hidy, G. M., Blanchard, C. L., Baumann, K., Edgerton, E., Tanenbaum, S., Shaw, S., Knipping,
1022 E., Tombach, I., Jansen, J., and Walters, J.: Chemical climatology of the southeastern
1023 United States, 1999-2013, *Atmos. Chem. Phys.*, 14, 11893-11914, doi:10.5194/acp-14-
1024 11893-2014, 2014.

1025 Hodzic, A., and Jimenez, J. L.: Modeling anthropogenically controlled secondary organic
1026 aerosols in a megacity: a simplified framework for global and climate models, *Geosci.*
1027 *Model Dev.*, 4, 901-917, doi:10.5194/gmd-4-901-2011, 2011.

1028 Holben, B. N., Eck, T. F., Slutsker, I., Tanre, D., Buis, J. P., Setzer, A., Vermote, E., Reagan, J.
1029 A., Kaufman, Y. J., Nakajima, T., Lavenu, F., Jankowiak, I., and Smirnov, A.:
1030 AERONET – A federated instrument network and data archive for aerosol
1031 characterization, *Remote Sens. Environ.*, 66, 1-16, doi:10.1016/S0034-4257(98)00031-5.,
1032 1998.

1033 Hoyle, C., Boy, M., Donahue, N. M., Fry, J. L., Glasius, M., Guenther, A., Hallar, A. G., Huff
1034 Hartz, K., Petters, M. D., Petaja, T., Rosenoern, T., and Sullivan, A. P.: A review of the
1035 anthropogenic influence on biogenic secondary organic aerosol, *Atmos. Chem. Phys.*, 11,
1036 321-343, doi:10.5194/acp-11-321-2011, 2011.

1037 Hu, W., Campuzano-Jost, P., Palm, B. B., Day, D. A., Ortega, A. M., Hayes, P. L., Krechmer, J.
1038 E., Chen, Q., Kuwata, M., Liu, Y. J., de Sa, S. S., Martin, S. T., Hu, M., Budisulistiorini,
1039 S. H., Riva, M., Surratt, J. D., St. Clair, J. M., Isaacman-Van Wertz, G., Yee, L. D.,
1040 Goldstein, A. H., Carbone, S., Artaxo, P., de Gouw, J. A., Koss, A., Wisthaler, A.,
1041 Mikoviny, T., Karl, T., Kaser, L., Jud, W., Hansel, A., Docherty, K. S., Robinson, N. H.,
1042 Coe, H., Allan, J. D., Canagaratna, M. R., Paulot, F., and Jimenez, J. L.: Characterization
1043 of a real-time tracer for isoprene epoxydiols-derived secondary organic aerosol (IEPOX-
1044 SOA) from aerosol mass spectrometer measurements, *Atmos. Chem. Phys. Discuss.*, 15,
1045 11223-11276, doi:10.5194/acpd-15-11223-2015, 2015.

1046 Hu, X., Walker, L. A., Lyapustin, A., Wang, Y., and Liu, Y.: 10-year spatial and temporal trends
1047 of PM_{2.5} concentrations in the southeastern US estimated using high-resolution satellite
1048 data, *Atmos. Chem. Phys.*, 14, 6301-6314, doi:10.5194/acp-14-6301-2014, 2014.

1049 Hu, L., Millet, D. B., Baasandorj, M., Griffis, T. J., Turner, P., Helmig, D., Curtis, A. J., and
1050 Hueber, J.: Isoprene emissions and impacts over an ecological transition region in the US
1051 Upper Midwest inferred from tall tower measurements, *J. Geophys. Res.*, in press,
1052 doi:10.1002/2014JD022732, 2015.

1053 Hudman, R. C., Moore, N. E., Mebust, A. K., Martin, R. V., Russell, A. R., Valin, L. C. and
1054 Cohen, R. C.: Steps towards a mechanistic model for global soil nitric oxide emissions:
1055 implementation and space-based constraints, *Atmos. Chem. Phys.*, 12, 7770 – 7795,
1056 doi:10.5194/acp-12-7779-2012, 2012.

1057 Jacob, D. J., Horowitz, L. W., Munger, J. W., Heikes, B. G., Dickerson, R. R., Artz, R. S. and
1058 Keene, W. C.: Seasonal transition from NO_x- to hydrocarbon-limited conditions for
1059 ozone production over the eastern United States in September, *J. Geophys. Res.*,
1060 100(D5), 9315-9324, doi:10.1029/94JD03125, 1995.

1061 Jaegle, L., Quinn, P. K., Bates, T. S., Alexander, B., and Lin, J.-T.: Global distribution of sea salt
1062 aerosols: new constraints from in situ and remote sensing observations, *Atmos. Chem.*
1063 *Phys.*, 11, 3137-3157, doi:10.5194/acp-11-3137-2011, 2011.

1064 Jenkin, M. E., Saunders, S. M., and Pilling, M. J.: The tropospheric degradation of volatile
1065 organic compounds: A protocol for mechanism development, *Atmos. Environ.*, 31, 81-
1066 104, doi:10.1016/s1352-2310(96)00105-7, 1997.

1067 Jimenez, J. L., Canagaratna, M. R., Donahue, N. M., Prevot, A. S. H., Zhang, Q., Kroll, J. H.,
1068 DeCarlo, P. F., Allan, J. D., Coe, H., Ng, N. L., Aiken, A. C., Docherty, K. S., Ulbrich, I.
1069 M., Grieshop, A. P., Robinson, A. L., Duplissy, J., Smith, J. D., Wilson, K. R., Lanz, V.
1070 A., Hueglin, C., Sun, Y. L., Tian, J., Laak-sonen, A., Raatikainen, T., Rautiainen, J.,
1071 Vaattovaara, P., Ehn, M., Kulmala, M., Tomlinson, J. M., Collins, D. R., Cubison, M. J.,
1072 Dunlea, E. J., Huffman, J. A., Onasch, T. B., Alfarra, M. R., Williams, P. I., Bower, K.,
1073 Kondo, Y., Schneider, J., Drewnick, F., Borrmann, S., Weimer, S., Demerjian, K.,
1074 Salcedo, D., Cottrell, L., Griffin, R., Takami, A., Miyoshi, T., Hatakeyama, S.,
1075 Shimono, A., Sun, J. Y., Zhang, Y. M., Dzepina, K., Kimmel, J. R., Sueper, D., Jayne, J.
1076 T., Herndon, S. C., Trimborn, A. M., Williams, L. R., Wood, E. C., Middlebrook, A. M.,
1077 Kolb, C. E., Baltensperger, U., and Worsnop, D. R.: Evolution of organic aerosols in the
1078 Atmosphere, *Science*, 326, 1525–1529, doi:10.1126/science.1180353, 2009.

1079 Jolleys, M. D., Coe, H., McFiggans, G., Capes, G., Allan, J. D., Crosier, J., Williams, P. I., Allen,
1080 G., Bower, K. N., Jimenez, J. L., Russell, L. M., Grutter, M., and Baumgardner, D.:
1081 Characterizing the aging of biomass burning organic aerosol by use of mixing ratios: a
1082 meta-analysis of four regions, *Environ. Sci. Technol.*, 46, 13093-13102,
1083 doi:10.1021/es302386v, 2012.

1084 Kim, P. S., Jacob, D. J., Liu, X., Warner, J. X., Yang, K., Chance, K., Thouret, V., and Nedelec,
1085 P.: Global ozone-CO correlations from OMI and AIRS: constraints on tropospheric ozone
1086 sources, *Atmos. Chem. Phys.*, 13, 9321-9335, doi:10.5194/acp-13-9321-2013, 2013.

1087 Kleindienst, T. E., Jaoui, M., Lewandowski, M., Offenber, J. H., Lewis, C. W., Bhave, P. V.,
1088 and Edney, E. O.: Estimates of the contributions of biogenic and anthropogenic
1089 hydrocarbons to secondary organic aerosol at a southeastern US location, *Atmos.*
1090 *Environ.*, 41, 8288-8300, doi:10.1016/j.atmosenv.2007.06.045, 2007.

1091 Kleinman, L. I.: Seasonal dependence of boundary layer peroxide concentration: The low and
1092 high NO_x regimes, *J. Geophys. Res.*, 96(D11), 20721 – 20733, doi:10.1029/91JD02040,
1093 1991.

1094 Koepke P., Hess, M., Schult, I., and Shettle, E. P.: Global Aerosol Data Set, Max-Planck-Institut
1095 fur Meteorologie, Hamburg, 1997.

1096 Kroll, J. H., Ng, N. L., Murphy, S. M., Flagan, R. C., and Seinfeld, J. H.: Secondary organic
1097 aerosol formation from isoprene photooxidation under high-NO_x conditions, *Geophys.*
1098 *Res. Lett.*, 32, L18808, doi:10.1029/2005GL023637, 2005.

1099 Kroll, J. H., Ng, N. L., Murphy, S. M., Flagan, R. C., and Seinfeld, J. H.: Secondary organic
1100 aerosol formation from isoprene photooxidation, *Environ. Sci. Technol.*, 40, 1869-1877,
1101 doi:10.1021/es0524301, 2006.

1102 Langridge, J. M., Richardson, M. S., Lack, D., Law, D., and Murphy, D. M.: Aircraft instrument
1103 for comprehensive characterization of aerosol optical properties, Part I: Wavelength-
1104 dependent optical extinction and its relative humidity dependence measured using cavity
1105 ringdown spectroscopy, *Aerosol Sci. Technol.*, 45(11), 1305:1318,
1106 doi:10.1080/02786826.2011.592745, 2011.

1107 Leibensperger, E. M., Mickley, L. J., Jacob, D. J., Chen, W.-T., Seinfeld, J. H., Nenes, A.,
1108 Adams, P. J., Streets, D. G., Kumar, N., and Rind, D.: Climatic effects of 1950-2050
1109 changes in US anthropogenic aerosols – Part I: Aerosol trends and radiative forcing,
1110 *Atmos. Chem. Phys.*, 12, 3333-3348, doi:10.5194/acp-12-3333-2012, 2012a.

1111 Leibensperger, E. M., Mickley, L. J., Jacob, D. J., Chen, W.-T., Seinfeld, J. H., Nenes, A.,
1112 Adams, P. J., Streets, D. G., Kumar, N., and Rind, D.: Climatic effects of 1950-2050

- 1113 changes in US anthropogenic aerosols – Part 2: Climate response, *Atmos. Chem. Phys.*,
1114 12, 3349-3362, doi:10.5194/acp-12-3349-2012, 2012b.
- 1115 Levy, R. C., Mattoo, S., Munchak, L. A., Remer, L. A., Sayer, A. M., Patadia, F., and Hsu, N. C.:
1116 The Collection 6 MODIS aerosol products over land and ocean, *Atmos. Meas. Tech.*, 6,
1117 2989-3034, doi:10.5194/amt-6-2989-2013, 2013.
- 1118 Li, J., Ying, Q., Yi, B., and Yang, P.: Role of stabilized Criegee Intermediates in the formation of
1119 atmospheric sulfate in eastern United States, *Atmos. Environ.*, 79, 442-447,
1120 doi:10.1016/j.atmosenv.2013.06.048, 2013.
- 1121 Liao, J., Froyd, K. D., Murphy, D. M., Keutsch, F. N., Yu, G., Wennberg, P. O., St. Clair, J. M.,
1122 Crounse, J. D., Wisthaler, A., Mikoviny, T., Jimenez, J. L., Campuzano-Jost, P., Day, D.
1123 A., Hu, W., Ryerson, T. B., Pollack, I. B., Peischl, J., Anderson, B. E., Ziemba, L. D.,
1124 Blake, D. R., Meinardi, S., and Diskin, G.: Airborne measurements of organosulfates
1125 over the continental U. S., *J. Geophys. Res.*, 120, doi:10.1002/2014JD022378, 2015.
- 1126 Liggio, J., Li, S.-M., Vlasenko, A., Stroud, C., and Makar, P.: Depression of ammonium uptake to
1127 sulfuric acid aerosols by competing uptake of ambient organic gases, *Environ. Sci.*
1128 *Technol.*, 45, 2790-2796, doi:10.1021/es103801g, 2011.
- 1129 Lim, H.-J., and Turpin, B. J.: Origins of primary and secondary organic aerosol in Atlanta: results
1130 of time-resolved measurements during the Atlanta Supersite Experiment, *Environ. Sci.*
1131 *Technol.*, 36, 4489-4496, doi:10.1021/es0206487, 2002.
- 1132 [Lin, J.-T., and McElroy, M. B.: Impacts of boundary layer mixing on pollutant vertical profiles in
1133 the lower troposphere: Implications to satellite remote sensing, *Atmos. Environ.*, 44,
1134 1726-739, doi:10.1016/j.atmosenv.2010.02.009, 2010.](#)
- 1135 Liu, D., Wang, Z., Liu, Z., Winker, D., and Trepte, C.: A height resolved global view of dust
1136 aerosols from the first year CALIPSO lidar measurements, *J. Geophys. Res.*, 113,
1137 D16214, doi:10.1029/2007JD009776, 2008.
- 1138 Liu, H., Jacob, D. J., Bey, I., and Yantosca, R. M.: Constraints from ^{210}Pb and ^7Be on wet
1139 deposition and transport in a global three-dimensional chemical tracer model driven by
1140 assimilated meteorological fields, *J. Geophys. Res.*, 106(D11), 12109–12128,
1141 doi:10.1029/2000JD900839, 2001.
- 1142 Liu Y., Park, R. J., Jacob, D. J., Li, Q., Kilaru, V., and Sarnat, J. A.: Mapping annual mean
1143 ground-level $\text{PM}_{2.5}$ concentrations using Multiangle Imaging Spectroradiometer aerosol
1144 optical thickness over the contiguous United States, *J. Geophys. Res.*, 109, D22206,
1145 doi:10.1029/2004JD005025, 2004.

Patrick 8/27/2015 11:44 AM

Deleted: 106

1147 Mao, J., Paulot, F., Jacob, D. J., Cohen, R. C., Crouse, J. D., Wennberg, P. O., Keller, C. A.,
1148 Hudman, R. C., Barkley, M. P., and Horowitz, L. W.: Ozone and organic nitrates over the
1149 eastern United States: Sensitivity to isoprene chemistry, *J. Geophys. Res. Atmos.*, 118,
1150 11256-11268, doi:10.1002/jgrd/50817, 2013.

1151 Malm, W. C., Sisler, J. F., Huffman, D., Eldred, R. A., and Cahill, T. A.: Spatial and seasonal
1152 trends in particle concentration and optical extinction in the United States, *J. Geophys.*
1153 *Res.*, 99(D1), 1347-1370, doi:10.1029/93JD02916, 1994.

1154 Marais, E., et al.: A mechanistic model of isoprene aerosol formation for improved understanding
1155 of organic aerosol composition, presented at the SEAC⁴RS Science Team Meeting,
1156 Pasadena, Calif., 28 Apr – 1 May, 2015.

1157 Martin, R. V., Jacob, D. J., Yantosca, R. M., Chin, M., and Ginoux, P.: Global and regional
1158 decreases in tropospheric oxidants from photochemical effects of aerosols, *J. Geophys.*
1159 *Res.*, 108, 4097, doi:10.1029/2002JD002622, 2003.

1160 Martin, S. T., Hung, H.-H., Park, R. J., Jacob, D. J., Spurr, R. J. D., Chance, K. V., and Chin, M.:
1161 Effects of the physical state of tropospheric ammonium-sulfate-nitrate particles on global
1162 aerosol direct radiative forcing, *Atmos. Chem. Phys.*, 4, 183-214, doi:10.5194/acp-4-183-
1163 2004, 2004.

1164 Mauldin III, R. L., Berndt, T., Sipila, M., Paasonen, P., Petaja, T., Kim, S., Kurten, T., Stratmann,
1165 F., Kerminen, V.-M., and Kulmala, M.: A new atmospherically relevant oxidant of
1166 sulphur dioxide, *Nature*, 488, 193-196, doi:10.1038/nature11278, 2012.

1167 McKeen, S., Chung, S. H., Wilczak, J., Grell, G., Djalalova, I., Peckham, S., Gong, W., Bouchet,
1168 V., Moffet, R., Tang, Y., Carmichael, G. R., Mathur, R., and Yu, S.: Evaluation of
1169 several PM_{2.5} forecast models using data collected during the ICARTT/NEAQS 2004
1170 field study, *J. Geophys. Res.*, 112, D10S20, doi:10.1029/2006JD007608, 2007.

1171 McNeill, V. F., Woo, J. L., Kim, D. D., Schwier, A. N., Wannell, N. J., Sumner, A. J., and
1172 Barakat, J. M.: Aqueous-phase secondary organic aerosol and organosulfate formation in
1173 atmospheric aerosols: a modeling study, *Environ. Sci. Technol.*, 46, 8075-8081,
1174 doi:10.1021/es3002986, 2012.

1175 Millet, D. B., Baasandorj, M., Farmer, D. K., Thornton, J. A., Baumann, K., Brophy, P.,
1176 Chaliyakunnel, S., de Gouw, J. A., Graus, M., Hu, L., Koss, A., Lee, B. H., Lopez-
1177 Hilfiker, F. D., Neuman, J. A., Paulot, F., Peischl, J., Pollack, I. B., Ryerson, T. B.,
1178 Warneke, C., Williams, B. J., and Xu, J.: A large and ubiquitous source of atmospheric
1179 formic acid, *Atmos. Chem. Phys. Discuss.*, 15, 4537-4599, doi:10.5194/acpd-15-4537-
1180 2015, 2015.

1181 Murphy, B. N., Donahue, N. M., Fountoukis, C., Dall'Osto, M., O'Dowd, C., Kiendler-Scharr,
1182 A., and Pandis, S. N.: Functionalization and fragmentation during ambient organic
1183 aerosol aging: application of the 2-D volatility basis set to field studies, *Atmos. Chem.*
1184 *Phys.*, 12, 10797-10816, doi:10.5194/acp-12-10797-2012, 2012.

1185 Murphy, D. M., Cziczo, D. J., Froyd, K. D., Hudson, P. K., Matthew, B. M., Middlebrook, A. M.,
1186 Peltier, R. E., Sullivan, A., Thomson, D. S., and Weber, R. J.: Single-particle mass
1187 spectrometry of tropospheric aerosol particles, *J. Geophys. Res.*, 111, D23S32,
1188 doi:10.1029/2006JD007340, 2006.

1189 NADP: National Atmospheric Deposition Program Animated Maps, Available at:
1190 <http://nadp.sws.uiuc.edu/data/animaps.aspx>, Accessed: March 7, 2015, 2015.

1191 Newland, M. J., Rickard, A. R., Alam, M. S., Vereecken, L., Munoz, A., Rodenas, M., and Bloss,
1192 W. J.: Kinetics of stabilised Criegee intermediates derive from alkene ozonolysis:
1193 reactions with SO₂, H₂O and decomposition under boundary layer conditions, *Phys.*
1194 *Chem. Chem. Phys.*, 17, 4076-4088, doi:10.1039/c4cp04186k, 2014.

1195 NOAA National Climatic Data Center: State of the Climate: Wildfires for Annual 2011,
1196 published online December 2011, retrieved on March 26, 2015 from
1197 <http://www.ncdc.noaa.gov/sotc/fire/2011/13>, 2011.

1198 Pankow, J. F.: An absorption model of gas/particle partitioning of organic compounds in the
1199 atmosphere, *Atmos. Environ.*, 28, 185-188, doi:10.1016/1352-2310(94)90093-0, 1994.

1200 Park, R. J., Jacob, D. J., Chin, M., and Martin, R. V.: Sources of carbonaceous aerosols over the
1201 United States and implications for natural visibility, *J. Geophys. Res.*, 108(D12), 4355,
1202 doi:10.1029/2002JD003190, 2003.

1203 Park, R. J., Jacob, D. J., Field, B. D., Yantosca, R. M., and Chin, M.: Natural and transboundary
1204 pollution influences on sulfate-nitrate-ammonium aerosols in the United States:
1205 Implications for policy, *J. Geophys. Res.*, 109, D15204, doi:10.1029/2003JD004473,
1206 2004.

1207 Park, R. J., Jacob, D. J., Kumar, N., and Yantosca, R. M.: Regional visibility statistics in the
1208 United States: Natural and transboundary pollution influences, and implications for the
1209 Regional Haze Rule, *Atmos. Environ.*, 40, 5405-5423,
1210 doi:10.1016/j.atmosenv.2006.04.059, 2006.

1211 Park, R. J., Jacob, D. J., and Logan, J. A.: Fire and biofuel contributions to annual mean aerosol
1212 mass concentrations in the United States, *Atmos. Environ.*, 41, 7389-7400,
1213 doi:10.1016/j.atmosenv.2007.05.061, 2007.

1214 Paulot, F., Jacob, D. J., Pinder, R. W., Bash, J. O., Travis, K., and Henze, D. K.: Ammonia
1215 emissions in the United States, European Union, and China derived by high-resolution
1216 inversion of ammonium wet deposition data: Interpretation with a new agricultural
1217 emissions inventory (MASAGE_NH3), *J. Geophys. Res. Atmos.*, 119, 4343-4364,
1218 doi:10.1002/2013JD021130, 2014.

1219 Peterson, D. A., Hyer, E. J., Campbell, J. R., Fromm, M. D., Hair, J. W., Butler, C. F., and Fenn,
1220 M. A.: The 2013 Rim Fire: Implications for predicting extreme fire spread,
1221 pyroconvection, and smoke emissions, *Bull. Amer. Meteor. Soc.*, doi:10.1175/BAMS-D-
1222 14-00060.1, 2015.

1223 Pfister, L., Rosenlof, K., Ueyama, R., and Heath, N.: A meteorological overview of the SEAC⁴RS
1224 mission, presented at the SEAC⁴RS Science Team Meeting, Pasadena, Calif., 28 Apr – 1
1225 May, 2015.

1226 Pierce, J. R., Evans, M. J., Scott, C. E., D' Andrea, S. D., Farmer, D. K., Swietlicki, E., and
1227 Spracklen, D. V.: Weak global sensitivity of cloud condensation nuclei and aerosol
1228 indirect effect to Criegee + SO₂ chemistry, *Atmos. Chem. Phys.*, 13, 3163-3176,
1229 doi:10.5194/acp-13-3163-2013, 2013.

1230 Pye, H. O. T., Liao, H., Wu, S., Mickley, L. J., Jacob, D. J., Henze, D. K., and Seinfeld, J. H.:
1231 Effect of changes in climate and emissions on future sulfate-nitrate-ammonium aerosol
1232 levels in the United States, *J. Geophys. Res.*, 114, D01205, doi:10.1029/2008JD010701,
1233 2009.

1234 Pye, H. O. T., Chan, A. W. H., Barkley, M. P., and Seinfeld, J. H.: Global modeling of organic
1235 aerosol: the importance of reactive nitrogen (NO_x and NO₃), *Atmos. Chem. Phys.*, 10,
1236 11261-11276, doi:10.5194/acp-10-11261-2010, 2010.

1237 Remer, L. A., Kaufman, Y. J., Tanre, D., Mattoo, S., Chu, D. A., Martins, J. V., Li, R.-R., Ichoku,
1238 C., Levy, R. C., Kleidman, R. G., Eck, T. F., Vermote, E., and Holben, B. N.: The
1239 MODIS aerosol algorithm, products, and validation, *J. Atmos. Sci.*, 62, 947-973,
1240 doi:10.1175/jas3385.1, 2005.

1241 Russell, A. R., Valin, L. C., and Cohen, R. C.: Trends in OMI NO₂ observations over the United
1242 States: effects of emission control technology and the economic recession, *Atmos. Chem.*
1243 *Phys.*, 12, 12197-12209, doi:10.5194/acp-12-12197-2012, 2012.

1244 Saide, P. E., Peterson, D., da Silva, A., Anderson, B., Ziemba, L. D., Diskin, G., Sachse, G., Hair,
1245 J., Butler, C., Fenn, M., Jimenez, J. L., Campuzano-Jost, P., Perring, A., Schwarz, J.,
1246 Markovic, M. Z., Russell, P., Redemann, J., Shinzuka, Y., Streets, D. G., Yan, F., Dibb,
1247 J., Yokelson, R., Toon, O. B., Hyer, E., and Carmichael, G. R.: Revealing important

1248 nocturnal and day-to-day variations in fire smoke emissions through a novel
1249 multiplatform inversion, submitted.

1250 Sarwar, G., Simon, H., Fahey, K., Mathur, R., Goliff, W. S., and Stockwell, W. R.: Impact of
1251 sulfur dioxide oxidation by Stabilized Criegee Intermediate on sulfate, *Atmos. Environ.*,
1252 85, 204-214, doi:10.1016/j.atmosenv.2013.12.013, 2014.

1253 Saunders, S. M., Jenkin, M. E., Derwent, R. G., and Pilling, M. J.: Protocol for the development
1254 of the Master Chemical Mechanism, MCM v3 (Part A): Tropospheric degradation of
1255 non-aromatic volatile organic compounds, *Atmos. Chem. Phys.*, 3, 161-180,
1256 doi:10.5194/acp-3-161-2003, 2003.

1257 [Scarino, A. J., Oband, M. D., Fast, J. D., Burton, S. P., Ferrare, R. A., Hostetler, C. A., Berg, L.](#)
1258 [K., Lefer, B., Haman, C., Hair, J. W., Rogers, R. R., Butler, C., Cook, A. L., and Harper,](#)
1259 [D. B.: Comparison of mixed layer heights from airborne high spectral resolution lidar,](#)
1260 [ground-based measurements, and the WRF-Chem model during CalNex and CARES,](#)
1261 [Atmos. Chem. Phys., 14, 5547-5560, doi:10.5194/acp-14-5547-2014, 2014a.](#)

1262 [Scarino, A. J., Ferrare, R., Burton, S., Hostetler, C., Hair, J., Rogers, R., Berkoff, T., Collins, J.,](#)
1263 [Seaman, S., Cook, A., Harper, D., Sawamura, P., Randles, C., and daSilva, A.: Assessing](#)
1264 [aerosol mixed layer heights from the NASA LaRC airborne HSRL-2 during the](#)
1265 [DISCOVER-AQ Field Campaigns: Houston 2013, Abstract A31C-3040 presented at](#)
1266 [2014 Fall Meeting, AGU, San Francisco, Calif., 15-19 Dec. 2014b.](#)

1267 Schwarz, J. P., Perring, A. E., Markovic, M. Z., Gao, R. S., Ohata, S., Langridge, J., Law, D.,
1268 McLaughlin, R., and Fahey, D. W.: Technique and theoretical approach for quantifying
1269 the hygroscopicity of black-carbon-containing aerosol using a single particle soot
1270 photometer, *J. Aeros. Sci.*, 81, 110-126, doi:10.1026/j.jaerosci.2014.11.009, 2015.

1271 Sipila, M., Jokinen, T., Berndt, T., Richters, S., Makkonen, R., Donahue, N. M., Mauldin III, R.
1272 L., Kurten, T., Paasonen, P., Sarnela, N., Ehn, M., Junninen, H., Rissanen, M. P.,
1273 Thornton, J., Stratmann, F., Herrmann, H., Worsnop, D. R., Kulmala, M., Kerminen, V.-
1274 M., and Petaja, T.: Reactivity of stabilize Criegee intermediates (sCIs) from isoprene and
1275 monoterpene ozonolysis toward SO₂ and organic acids, *Atmos. Chem. Phys.*, 14, 12143-
1276 12153, doi:10.5194/acp-14-12143-2014, 2014.

1277 Solomon, P. A., Crumpler, D., Flanagan, J. B., Jayanty, R. K. M., Rickman, E. E., and McDade
1278 C. E.: U.S. National PM_{2.5} Chemical Speciation Monitoring Networks – CSN and
1279 IMPROVE: Description of Networks, *J. Air Waste Manage. Assoc.*, 64(12), 1410-1438,
1280 doi:10.1080/10962247.2014.956904, 2014.

1281 Spracklen, D. V., Jimenez, J. L., Carslaw, K. S., Worsnop, D. R., Evans, M. J., Mann, G. W.,
1282 Zhang, Q., Canagaratna, M. J., Allan, J., Coe, H., McFiggans, G., Rap, A., and Forster,
1283 P.: Aerosol mass spectrometer constraint on the global secondary organic aerosol budget,
1284 *Atmos. Chem. Phys.*, 11, 12109-12136, doi:10.5194/acp-11-12109-2011, 2011.

1285 St. Clair, J. M., McCabe, D. C., Crounse, J. D., Steiner, U., and Wennberg, P. O.: Chemical
1286 ionization tandem mass spectrometer for the in situ measurement of methyl hydrogen
1287 peroxide, *Rev. Sci. Instrum.*, 81, 094102-094106, doi:10.1063/1.3480552, 2010.

1288 Stone, D., Blitz, M., Daubney, L., Howes, N. U., and Seakins, P.: Kinetics of CH₂OO reactions
1289 with SO₂, NO₂, NO, H₂O, and CH₃CHO as a function of pressure, *Phys. Chem. Chem.*
1290 *Phys.*, 16, 1139-1149, doi:10.1039/c3cp54391a, 2014.

1291 Surratt, J. D., Kroll, J. H., Kleindienst, T. E., Edney, E. O., Claeys, M., Sorooshian, A., Ng, N. L.,
1292 Offenberg, J. H., Lewandowski, M., Jaoui, M., Flagan, R. C., and Seinfeld, J. H.:
1293 Evidence for organosulfates in secondary organic aerosol, *Environ. Sci., Tech.*, 41, 517-
1294 527, doi:10.1021/es062081q, 2007.

1295 Theil, H.: A rank-invariant method of linear and polynomial regression analysis, *Proc. Kon. Ned.*
1296 *Akad. V. Wetensch. A*, 53, 386-392, 1950.

1297 Thomson, D. S., Schein, M. E., and Murphy, D. M.: Particle analysis by laser mass spectrometry
1298 WB-57F instrument overview, *Aerosol Sci. Technol.*, 33(1-2), 153-169,
1299 doi:10.1080/027868200410903, 2000.

1300 Thornhill, K. L., Chen, G., Dibb, J., Jordan, C. E., Omar, A., Winstead, E. L., Schuster, G.,
1301 Clarke, A., McNaughton, C., Scheur, E., Blake, D., Sachse, G., Huey, L. G., Singh, H. B.,
1302 and Anderson, B. E.: The impact of local sources and long-range transport on aerosol
1303 properties over the northeast U.S. region during INTEX-NA, *J. Geophys. Res.*, 113,
1304 D08201, doi:10.1029/2007JD008666, 2008.

1305 Toon, O. B., et al.: Planning, implementation, and scientific goals of the Studies of Emissions and
1306 Atmospheric Composition, Clouds, and Climate Coupling by Regional Surveys
1307 (SEAC⁴RS) field mission, in prep.

1308 Travis, K., et al.: Declining NO_x in the Southeast US and implications for ozone-NO_x-VOC
1309 chemistry, presented at the SEAC⁴RS Science Team Meeting, Pasadena, Calif., 28 Apr –
1310 1 May, 2015.

1311 Tsigaridis, K., Daskalakis, N., Kanakidou, M., Adams, P. J., Artaxo, P., Bahadur, R., Balkanski,
1312 Y., Bauer, S. E., Bellouin, N., Benedetti, A., Bergman, T., Berntsen, T. K., Beukes, J. P.,
1313 Bian, H., Carslaw, K. S., Chin, M., Curci, G., Diehl, T., Easter, R. C., Ghan, S. J., Gong,
1314 S. L., Hodzic, A., Hoyle, C. R., Iversen, T., Jathar, S., Jimenez, J. L., Kaiser, J. W.,

1315 Kirkevåg, A., Koch, D., Kokkola, H., Lee, Y. H., Lin, G., Liu, X., Luo, G., Ma, X.,
1316 Mann, G. W., Mihalopoulos, N., Morcrette, J.-J., Müller, J.-F., Myhre, G.,
1317 Myriokefalitakis, S., Ng, S., O'Donnell, D., Penner, J. E., Pozzoli, L., Pringle, K. J.,
1318 Russell, L. M., Schulz, M., Sciare, J., Seland, Ø., Shindell, D. T., Sillman, S., Skeie, R.
1319 B., Spracklen, D., Stavrakou, T., Steenrod, S. D., Takemura, T., Tiitta, P., Tilmes, S.,
1320 Tost, H., van Noije, T., van Zyl, P. G., von Salzen, K., Yu, F., Wang, Z., Wang, Z.,
1321 Zaveri, R. A., Zhang, H., Zhang, K., Zhang, Q., and Zhang, X.: The AeroCom evaluation
1322 and intercomparison of organic aerosol in global models, *Atmos. Chem. Phys.*, 14,
1323 10845-10895, doi:10.5194/acp-14-10845-2014, 2014.

1324 Turquety, S., Logan, J. A., Jacob, D. J., Hudman, R. C., Leung, F. Y., Heald, C. L., Yantosca, R.
1325 M., Wu, S., Emmons, L. K., Edwards, D. P., and Sachse, G.: Inventory of boreal fire
1326 emissions for North America in 2004: the importance of peat burning and pyro-
1327 convective injections, *J. Geophys. Res.*, 112(D12), D12S03, doi:10.1029/2006JD007281,
1328 2007.

1329 van Donkelaar, A., Martin, R. V., Brauer, M., Kahn, R., Levy, R., Verduzco, C., and Villeneuve,
1330 P. J.: Global estimates of ambient fine particulate matter concentrations from satellite-
1331 based aerosol optical depth: development and application, *Environ. Health Perspect.*,
1332 118(6), 847-855, doi:10.1289/ehp.0901623, 2010.

1333 van Donkelaar, A., Martin, R. V., Pasch, A. N., Szykman, J. J., Zhang, L., Wang, Y. X., and
1334 Chen, D.: Improving the accuracy of daily-satellite-derived ground-level fine aerosol
1335 concentration estimates for North America, *Environ. Sci. Technol.*, 46, 11971-11978,
1336 doi:10.1021/es3025319, 2012.

1337 van Donkelaar, A., Martin, R. V., Spurr, R. J. D., Drury, E., Remer, L. A., Levy, R. C., and
1338 Wang, J.: Optimal estimation for global ground-level fine particulate matter
1339 concentrations, *J. Geophys. Res. Atmos.*, 118, 5621-5636, doi:10.1002/jgrd.50479, 2013.

1340 van Donkelaar, A., Martin, R. V., Brauer, M., and Boys, B. L.: Use of satellite observations for
1341 long-term exposure assessment of global concentrations of fine particulate matter,
1342 *Environ. Health Perspect.*, 123(2), 135-143, doi:10.1289/ehp.1408646, 2015.

1343 Wagner, N. L., Brock, C. A., Angevine, W. M., Beyersdorf, A., Campuzano-Jost, P., Day, D. A.,
1344 de Gouw, J. A., Diskin, G. S., Gordon, T. D., Graus, M. G., Huey, G., Jimenez, J. L.,
1345 Lack, D. A., Liao, J., Liu, X., Markovic, M. Z., Middlebrook, A. M., Mikoviny, T.,
1346 Peischl, J., Perring, A. E., Richardson, M. S., Ryerson, T. B., Schwarz, J. P., Warneke,
1347 C., Welti, A., Wisthaler, A., Ziemba, L. D., and Murphy, D. M.: In situ vertical profiles
1348 of aerosol extinction, mass, and composition over the southeast United States during

1349 SENEX and SEAC4RS: Observations of a modest aerosol enhancement aloft, *Atmos.*
1350 *Chem. Phys. Discuss.*, 15, 3127-3172, doi:10.5194/acpd-15-3127-2015, 2015.

1351 Walker, J. M., Philip, S., Martin, R. V., and Seinfeld J. H.: Simulation of nitrate, sulfate, and
1352 ammonium aerosols over the United States, *Atmos. Chem. Phys.*, 12, 11213-11227,
1353 doi:10.5194/acp-12-11213-2012, 2012.

1354 Wang, J., Jacob, D. J., and Martin, S. T.: Sensitivity of sulfate direct climate forcing to the
1355 hysteresis of particle phase transitions, *J. Geophys. Res.*, 113, D11207,
1356 doi:10.1029/2007JD009368, 2008.

1357 Wang, Q., Jacob, D. J., Spackman, J. R., Perring, A. E., Schwarz, J. P., Moteki, N., Marais, E. A.
1358 Ge, C., Wang, J., and Barrett, S. R. H.: Global budget and radiative forcing of black
1359 carbon aerosol: Constraints from pole-to-pole (HIPPO) observations across the Pacific, *J.*
1360 *Geophys. Res. Atmos.*, 119, 195-206, doi:10.1002/2013JD020824, 2014.

1361 Warneke, C., and the SENEX science team: Instrumentation and measurement strategy for the
1362 NOAA SENEX aircraft campaign as part of the Southeast Atmosphere Study 2013, to be
1363 submitted to *Atmos. Meas. Tech. Discuss.*, 2015.

1364 Washenfelder, R., Attwood, A. R., Brock, C. A., Guo, H., Xu, L., Weber, R. J., Ng, N. L., Allen,
1365 H. M., Ayres, B., Baumann, K., Cohen, R. C., Draper, D. C., Duffey, K. C., Edgerton, E.,
1366 Fry, J. L., Hu, W. W., Jimenez, J. L., Palm, B. B., Romer, P., Stone, E. A., Wooldridge,
1367 P. J., and Brown, S. S.: Biomass burning dominates brown carbon absorption in the rural
1368 southeastern United States, *Geophys. Res. Lett.*, 42, 653-664,
1369 doi:10.1002/2014GL062444, 2015.

1370 Weber, R. J., Sullivan, A. P., Peltier, R. E., Russell, A., Yan, B., Zheng, M., de Gouw, J.,
1371 Warneke, C., Brock, C., Holloway, J. S., Atlas, E. L., and Edgerton, E.: A study of
1372 secondary organic aerosol formation in the anthropogenic-influenced southeastern United
1373 States, *J. Geophys. Res.*, 112, D13302, doi:10.1029/2007JD008408, 2007.

1374 Welz, O., Savee, J. D., Osborn, D. L., Vasu, S. S., Percival, C. J., Shallcross, D. E., and Taatjes,
1375 C. A.: Direct kinetic measurements of Criegee Intermediate (CH_2OO) formed by reaction
1376 of CH_2I with O_2 , *Science*, 335, 204-207, doi:10.1126/science.1213229, 2012.

1377 Wolfe, G. M., Hanisco, T. F., Arkinson, H. L., Bui, T. P., Crouse, J. D., Dean-Day, J.,
1378 Goldstein, A., Guenther, A., Hall, S. R., Huey, G., Karl, T., Kim, P. S., Liu, X., Marvin,
1379 M. R., Mikoviny, T., Misztal, P., Nguyen, T. B., Peischl, J., Pollack, I., Ryerson, T., St.
1380 Clair, J. M., Teng, A., Travis, K. R., Wennberg, P. O., Wisthaler, A., and Ullmann, K.:
1381 Airborne flux observations provide novel constraints on sources and sinks of reactive
1382 gases in the lower atmosphere, submitted to *Science*, 2015.

1383 WRAP: Western Regional Air Partnership, Development of 2000-04 Baseline Period and 2018
1384 Projection Year Emission Inventories, Prepared by Air Sciences, Inc. Project No. 178-8,
1385 2005.

1386 Xu, L., Kollman, M. S., Song, C., Shilling, J. E., and Ng, N. L.: Effects of NO_x on the volatility
1387 of secondary organic aerosol from isoprene photooxidation, *Environ. Sci. Technol.*, 48,
1388 2253-2262, doi:10.1021/es404842g, 2014.

1389 Yu, K., et al.: Impact of grid resolution on tropospheric chemistry simulation constrained by
1390 observations from the SEAC⁴RS aircraft campaign, presented at the SEAC⁴RS Science
1391 Team Meeting, Pasadena, Calif., 28 Apr – 1 May, 2015.

1392 Yu, S., Dennis, R. L., Bhave, P. V., and Ender, B. K.: Primary and secondary organic aerosols
1393 over the United States: estimates on the basis of observed organic carbon (OC) and
1394 elemental carbon (EC), and air quality modeled primary OC/EC ratios, *Atmos. Environ.*,
1395 38, 5257-5268, doi:10.1016/j.atmosenv.2004.02.064, 2004.

1396 Zhang, H., Hoff, R. M., and Engel-Cox, J. A.: The relation between Moderate Resolution
1397 Imaging Spectroradiometer (MODIS) aerosol optical depth and PM_{2.5} over the United
1398 States: a geographical comparison by U.S. Environmental Protection Agency regions, *J.*
1399 *Air Waste Manage. Assoc.*, 59:11, 1358-1369, doi:10.3155/1047-3289.59.11.1358, 2009.

1400 Zhang, L., Gong, S., Padro, J., and Barrie, L.: A size-segregated particle dry deposition scheme
1401 for an atmospheric aerosol module, *Atmos. Environ.*, 35, 549-560, doi:10.1016/s1352-
1402 2310(00)00326-5, 2001.

1403 Zhang, L., Jacob, D. J., Knipping, E. M., Kumar, N., Munger, J. W., Carouge, C. C., van
1404 Donkelaar, A., Wang, Y. X., and Chen, D.: Nitrogen deposition to the United States:
1405 distribution, sources, and processes, *Atmos. Chem. Phys.*, 12, 4539-4554,
1406 doi:10.5194/acp-12-4539-2012, 2012.

1407 Zhang, Q., Jimenez, J. L., Canagaratna, M. R., Allan, J. D., Coe, H., Ulbrich, I., Alfarra, M. R.,
1408 Takami, A., Middlebrook, A. M., Sun, Y. L., Dzepina, K., Dunlea, E., Docherty, K., De-
1409 Carlo, P. F., Salcedo, D., Onasch, T., Jayne, J. T., Miyoshi, T., Shimojo, A.,
1410 Hatakeyama, S., Takegawa, N., Kondo, Y., Schneider, J., Drewnick, F., Borrmann, S.,
1411 Weimer, S., Demerjian, K., Williams, P., Bower, K., Bahreini, R., Cottrell, L., Griffin,
1412 R. J., Rautiainen, J., Sun, J. Y., Zhang, Y. M., and Worsnop, D. R.: Ubiquity and
1413 dominance of oxygenated species in organic aerosols in anthropogenically-influenced
1414 Northern Hemisphere midlatitudes, *Geophys. Res. Lett.*, 34, 6, L13801,
1415 doi:10.1029/2007gl029979, 2007.

1416 Zhang, X., Liu, Z., Hecobian, A., Zheng, M., Frank, N. H., Edgerton, E. S., and Weber, R. J.:
1417 Spatial and seasonal variations of fine particle water-soluble organic carbon (WSOC)
1418 over the southeastern United States: implications for secondary organic aerosol
1419 formation, *Atmos. Chem. Phys.*, 12, 6593-6607, doi:10.5194/acp-12-6593-2012, 2012.

1420 Zhu, L., et al.: Indirect validation of new OMI, GOME-2, and OMPS formaldehyde (HCHO)
1421 retrievals using SEAC⁴RS data, presented at the SEAC⁴RS Science Team Meeting,
1422 Pasadena, Calif., 28 Apr – 1 May, 2015.

1423 Zotter, P., El-Haddad, I., Zhang, Y., Hayes, P. L., Zhang, X., Lin, Y.-H., Wacker, L., Schnelle-
1424 Kreis, J., Abbaszade, G., Zimmerman, R., Surratt, J. D., Weber, R., Jimenez, J. L., Szidat,
1425 S., Baltensperger, U., and Prevot, A. S. H.: Diurnal cycle of fossil and nonfossil carbon
1426 using radiocarbon analyses during CalNex, *J. Geophys. Res. Atmos.*, 119, 6818-6835,
1427 doi:10.1002/2013JD021114, 2014.

1428
1429
1430
1431
1432
1433
1434
1435
1436
1437
1438
1439
1440
1441
1442
1443
1444
1445
1446
1447
1448
1449

1450 **Tables**

1451

1452 Table 1: Contiguous US (CONUS) Emissions for 2013^a

Source	NO _x [Tg N]	CO [Tg]	SO ₂ [Tg S]	NH ₃ [Tg]	BC [Tg]	OC [Tg]	Isoprene ^b [Tg C]	Monoterpenes ^b [Tg C]
Anthropogenic ^c	2.7 (0.07)	29.8 (0.65)	2.8 (0.14)	3.5 ^d (0.11)	0.26 (0.008)	0.58 (0.01)	-	-
Open Fires ^e	0.14 (0.004)	7.9 (0.21)	0.13 (0.002)	0.44 (0.008)	0.19 (0.003)	0.93 (0.01)	-	-
Soil ^f	0.69 (0.03)	-	-	-	-	-	-	-
Vegetation	-	-	-	0.17 (0.002)	-	-	12.2 (2.2)	4.1 (0.5)
Total	3.5 (0.11)	37.7 (0.85)	2.9 (0.14)	4.1 (0.12)	0.45 (0.01)	1.5 (0.02)	12.2 (2.2)	4.1 (0.5)

1453

1454 ^aAnnual totals. Emissions in the Southeast US for the two-month SEAC⁴RS period (August-
1455 September) are shown in parentheses. The Southeast US domain is as defined in Figure 2.

1456 ^bBiogenic VOC emissions are from the MEGAN2.1 inventory (Guenther et al., 2012) with
1457 isoprene emissions decreased by 15% (see text).

1458 ^cAnthropogenic emissions are from the EPA National Emissions Inventory (NEI08v2) scaled
1459 nationally to 2013 and with additional adjustments described in the text.

1460 ^dAgricultural ammonia emissions are from the MASAGE inventory on a 2° x 2.5° grid (Paulot et
1461 al., 2014), and are distributed on the 0.25° x 0.3125° grid following NEI08v2 as described in the
1462 text.

1463 ^eOpen fire emissions are from the Quick Fire Emissions Dataset (Darmanov and da Silva, 2013),
1464 with adjustments described in the text.

1465 ^fSoil and fertilizer NO_x emissions are from the BDSNP algorithm (Hudman et al., 2012).
1466 Fertilizer emissions are included in the anthropogenic total.

1467

1468

1469

1470

1471

1472

1473

1474 **Figure Captions**

1475

1476 Figure 1: Summertime and wintertime trends in mean surface $PM_{2.5}$ in the Southeast US for 2003-
1477 2013. Seasonal averages for each component are calculated by combining data from the EPA
1478 CSN and IMPROVE networks over the Southeast US domain defined in Figure 2. Ammonium is
1479 only measured by CSN. Organic aerosol (OA) and black carbon (BC) are only from IMPROVE
1480 because of change in the CSN measurement protocol over the 2003-2013 period and differences
1481 in the OA measurements between the two networks (see text for details). OA is inferred here
1482 from measured organic carbon (OC) using an OA/OC mass ratio of 2.24 as measured by the
1483 Aerodyne Aerosol Mass Spectrometer (AMS) in the boundary layer over the Southeast US. Note
1484 the different scales in different panels (sulfate and OA contribute most of $PM_{2.5}$). Trends are
1485 calculated using the Theil-Sen estimator (Theil, 1950) and are shown only if significant at the $\alpha =$
1486 0.05 level. Only the sulfate trend is significant in winter.

1487

1488 Figure 2: Flight tracks of the DC-8 aircraft during SEAC⁴RS superimposed on mean MEGAN2.1
1489 isoprene emissions for August-September 2013. The thick black line delineates the Southeast US
1490 domain as defined in this paper [95° W – 81.5° W, 30.5° N – 39° N].

1491

1492 Figure 3: Mean $PM_{2.5}$ in the Southeast US in August-September 2013. EPA observations (circles)
1493 are compared to GEOS-Chem model values (background). Model values are calculated at 35%
1494 relative humidity as per the Federal Reference Method protocol. Observed mean $PM_{2.5}$ speciation
1495 by mass is shown in the pie charts for representative CSN sites. Organic aerosol (OA) mass
1496 concentrations are derived from measurements of organic carbon (OC) by assuming an OA/OC
1497 mass ratio of 2.24.

1498

1499 Figure 4: Mean sulfate (top) and OC (bottom) surface air concentrations in the Southeast US in
1500 August-September 2013. Network observations from CSN (circles), IMPROVE (squares), and
1501 SEARCH (triangles) are compared to GEOS-Chem model values (background). OC
1502 measurements are artifact-corrected as described in the text. Source attribution for sulfate and OC
1503 is shown at right as averages for the Southeast US domain defined in Figure 2. For sulfate, source
1504 attribution is by SO_2 oxidant. For OC, source attribution is primary or secondary, by source type,
1505 and by NO regime.

1506

1507 Figure 5: Median vertical profiles of aerosol concentrations over the Southeast US (Figure 2)
1508 during the SEAC⁴RS aircraft campaign (August-September 2013). Observed and simulated
1509 profiles of sulfate (left), OA (center), and dust (right) in 1-km bins are shown with the
1510 corresponding median surface network observations. OC from the surface networks is converted
1511 to OA using an OA/OC ratio of 2.24. The contributions of anthropogenic SOA, biogenic SOA,
1512 and open fire POA to total simulated OA are also shown. The individual observations are shown
1513 in gray and the horizontal bars denote the 25th and 75th percentiles of the observations.
1514 Concentrations are in $\mu\text{g m}^{-3}$ converted to STP conditions for the aircraft data and under local
1515 conditions for the surface data. The choice of scale truncates some very large individual
1516 observations.

1517

1518 Figure 6: Median vertical profiles of aerosol composition over the Southeast US during
1519 SEAC⁴RS (August-September 2013). Observations from the DC-8 aircraft (left) are compared to
1520 GEOS-Chem values sampled at the aircraft times and locations (center). Also shown is the
1521 observed and simulated fraction of the total aerosol mass column below a given height (right).
1522 The Southeast US domain is as defined in Figure 2.

1523

1524 Figure 7: Extent of neutralization of sulfate aerosol in the Southeast US (August-September
1525 2013). The extent of neutralization for an external sulfate-nitrate-ammonium (SNA) mixture is
1526 given by the $f = [\text{NH}_4^+]/(2[\text{SO}_4^{2-}] + [\text{NO}_3^-])$ molar ratio, and this can be adjusted for an internal
1527 mixture by considering additional ions. The top panels show observations from the CSN network
1528 assuming an external (left) or internal (right) mixture; there is little difference between the two
1529 because the concentrations of additional ions are usually small. The bottom panels show the
1530 SEAC⁴RS aircraft observations below 2 km and corresponding GEOS-Chem values. Also shown
1531 are the lines corresponding to different extents of neutralization ($f = 0.5$ for ammonium bisulfate
1532 and $f = 1$ for ammonium sulfate).

1533

1534 **Figure 8:** Median vertical profiles of aerosol extinction coefficients (532 nm) over the Southeast
1535 US during SEAC⁴RS. The left panel shows independent observations from the NASA HSRL and
1536 NOAA CRDS instruments, with GEOS-Chem sampled at the times and locations of the available
1537 instrument data. The individual CRDS observations are shown in gray and the horizontal bars
1538 denote the 25th and 75th percentiles of the CRDS observations for each 1-km bin. The choice of
1539 scale truncates some very large individual observations. The right panel shows the observed

Patrick 8/27/2015 11:44 AM

Formatted: Font color: Auto

Patrick 8/27/2015 11:44 AM

Formatted: Justified

Patrick 8/27/2015 11:44 AM

Deleted: Figure 8: Correlation of the neutralization fraction bias in GEOS-Chem with organic aerosol (OA) concentrations. The ordinate shows the difference between simulated and observed extent of neutralization ($f = [\text{NH}_4^+]/(2[\text{SO}_4^{2-}] + [\text{NO}_3^-])$) in molar units along the SEAC⁴RS flight tracks in the Southeast US below 1 km. OA is from the aircraft observations. The regression coefficients shown inset are calculated using reduced major axis (RMA) regression and the correlation coefficient is shown with a 95% confidence interval calculated by bootstrapping with replacement with 1000 iterations. [2]

1553 (CRDS) and simulated fraction of the total AOD below a given height. The Southeast US domain
1554 is as defined in Figure 2.

1555

1556 | Figure 9: Mean aerosol optical depths (AODs) over the Southeast US during SEAC⁴RS (August-
1557 September 2013). AERONET data are shown as circles and are the same in all panels. The top
1558 panels show MODIS and MISR satellite observations with comparison statistics to AERONET
1559 | (correlation coefficients, numerical mean biases or NMBs, of collocated observations in time and
1560 | space). The bottom panels show GEOS-Chem model values sampled at the same locations and
1561 | times as the satellite retrievals. The noise in the MISR panels reflects infrequent sampling (9-day
1562 | return time, compared to 1-day for MODIS). The negative NMB for the MODIS data reflects
1563 | occasional retrievals of negative AOD.

1564

1565 | Figure 10: Seasonal variation of MODIS AOD over the Southeast US for 2006-2013. The
1566 | Southeast US domain is as defined in Figure 2.

1567

1568 | Figure 11: Seasonal transition of aerosol optical depth (AOD) and related variables over the
1569 | Southeast US in August-October 2013. (A) AODs measured by MODIS and AERONET, and
1570 | GEOS-Chem values sampled at AERONET times and locations with simulated contributions
1571 | from sulfate and OA. (B) 24-h average MEGAN2.1 isoprene emissions and GEOS-FP surface air
1572 | temperatures. (C) H₂O₂ concentrations measured from the aircraft below 1 km altitude and
1573 | simulated by GEOS-Chem sampled at the times and locations of the observations. Each data
1574 | point represents the median value over the Southeast US for an individual flight. GEOS-Chem
1575 | H₂O₂ concentrations averaged over the entire region (i.e. without sampling along the flight tracks)
1576 | are shown separately and extend into October. (D) Same as (C) but for the molar ratio of isoprene
1577 | peroxides (ISOPOOH) to isoprene nitrates (ISOPN). The Southeast US domain is as defined in
1578 | Figure 2.

1579

1580 | Figure 12: Seasonal aerosol cycle in the Southeast US in 2013. (Top) Daily mean EPA and
1581 | GEOS-Chem PM_{2.5}. (Middle) Daily maximum mixed layer height from GEOS-FP with 40%
1582 | downward correction applied year-round as in GEOS-Chem (see Section 2). (Bottom) Daily
1583 | mean AOD from MODIS and GEOS-Chem. GEOS-Chem results in this figure are from the
1584 | coarse-resolution (4° x 5°) global simulation for 2013. Smoothed curves are calculated using a
1585 | low-pass filter. All values are averaged over the Southeast US as defined in Figure 2.

Patrick 8/27/2015 11:44 AM

Deleted: 10

Patrick 8/27/2015 11:44 AM

Deleted:).

Patrick 8/27/2015 11:44 AM

Deleted: 11

Patrick 8/27/2015 11:44 AM

Deleted: 12

Patrick 8/27/2015 11:44 AM

Deleted: 13